Spring 5-2017

# Ab Initio Computation of Radiative Properties of Monatomic Hydrogen

Fanny Thomas
*Embry-Riddle Aeronautical University*

AB INITIO COMPUTATION OF RADIATIVE PROPERTIES OF MONATOMIC

HYDROGEN


A Thesis

Submitted to the Faculty

of

Embry-Riddle Aeronautical University

by

Fanny Thomas


In Partial Fulfillment of the

Requirements for the Degree

of

Master of Science in Aerospace Engineering


May 2017

Embry-Riddle Aeronautical University

Daytona Beach, Florida

AB INITIO COMPUTATION OF RADIATIVE PROPERTIES OF MONATOMIC

HYDROGEN

by

Fanny Thomas

A Thesis prepared under the direction of the candidate's committee chairman, Dr. Eric Perrell, Department of Aerospace Engineering, and has been approved by the members of the thesis committee. It was submitted to the School of Graduate Studies and Research and was accepted in partial fulfillment of the requirements for the degree of Master of Science in Aerospace Engineering.

THESIS COMMITTEE

_____
Chairman, Dr. Eric Perrell

_____
Member, Dr. Narayanaswami

_____
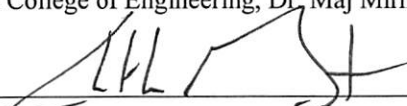Member, Dr. Engblom

_____
Graduate Program Coordinator, Dr. Magdy Attia

_____
Dean of College of Engineering, Dr. Maj Mirmirani

_____
Vice Chancellor, Academic Support, Dr. Christopher Grant


4.4.2017
Date

4/4/2017
Date

4/4/2017
Date

ACKNOWLEDGMENTS

## TABLE OF CONTENTS

## LIST OF TABLES

LIST OF FIGURES

## SYMBOLS

| | |
|---|---|
| $m$ | Mass |
| $v$ | Velocity |
| $k_R$ | Absorption Coefficient |
| $I$ | Intensity, $erg/s \cdot cm^2 \cdot sr$ |
| $q$ | Heat Flux |
| $\beta_R$ | Radiative Thermal Conductivity |
| $c$ | Speed of Light, $2.9979 \times 10^{10} \ cm/s$ |
| $A_{UL}$ | Einstein A Coefficient |
| $B_{UL} \ or \ B_{LU}$ | Einstein B Coefficient |
| $E$ | Energy |
| $h$ | Planck Constant, $6.6262 \times 10^{-27} \ erg \cdot s$ |
| $v$ | Radiation Frequency, $1/s$ |
| $\lambda$ | Wavelength, $mm$ |
| $\varepsilon_\lambda$ | Spontaneous Spectral Emission, $W/cm^3 \cdot mm \cdot sr$ |
| $n_U$ | Number Density of Atom At Upper Level |
| $n_L$ | Number Density of Atom At Lower Level |
| $\phi_\lambda$ | Line Broadening Function, $mm$ |
| $I_v$ | Spectral Intensity |
| $U$ | Upper level |
| $L$ | Lower level |
| $\rho$ | Linear momentum |
| $c_0$ | Speed of light in the gas |
| $\hbar$ | Reduced Planck's constant, $1.0546 \times 10^{-34} \ J \cdot s$ |
| $\varepsilon_0$ | Vacuum permittivity, $8.8542 \times 10^{-12} \ C^2/J \cdot m$ |
| $a_0$ | Bohr's radius, $5.2918 \times 10^{-11} \ m$ |
| $Z$ | Arbitrary atomic number |

ABBREVIATIONS

| CFD | Computational Fluid Dynamics |
|---|---|
| NEQAIR | Nonequilibrium Air Radiation code |
| HARA | Hypersonic Air Radiation Algorithm |
| LAPACK | Linear Algebra Package |
| BLAS | Basic Linear Algebra Subprograms |
| NIST | National Institute of Standards and Technology |

ABSTRACT

Thomas, Fanny MSAE, Embry-Riddle Aeronautical University, Aug 2016. Ab Initio Computation of Radiative Properties of Monatomic Hydrogen.

With renewed interest in planetary atmospheric entry, descent, and landing, NASA has noted a need for improved physics modeling in computational fluid dynamics. Uncertainty in experimental data used in radiation heat transfer computations leads to "over-engineering" of entry body heat shields, at large weight and cost penalties. There is interest in developing hypersonic thermophysics models from the known "first principles" of physics.

A method for computing high temperature gas emissivity and absorptivity from quantum mechanics principles is developed. The Schroedinger wave equation is cast as a discretized matrix eigenvalue problem which is solved using the ERAU parallel supercomputer. The numerical solutions for the wave functions are then integrated to determine the Einstein coefficients for emission and absorption, and hence the gas properties are tabulated as functions of temperature and pressure.

All of the published works found thus far assume Dirichlet or von Neumann boundary conditions for the eigenvalue problem. At best this presumes a priori knowledge of the solution. In general it is incorrect. The novel boundary condition treatment used here admits simultaneous solution for several wave functions, unlike the "shooting methods" in most textbooks. Therefore the novel boundary condition treatment is used in this thesis.

The hydrogen atom is studied, as analytical solutions for verification exist. Numerical solutions have been completed and compare very well with analytical

solutions, and with experimental data maintained by National Institutes of Standards (NIST).

# 1. Introduction

## 1.1. Background

Hypersonic flow simulation is largely a matter of accounting for the kinetic, thermal, and chemical energies of the gas, and their exchange at extremely high rates. At entry speeds, temperatures are high enough that heat transfer by radiation becomes important in the overall energy balance. Absorptivity and emissivity depend upon the gas composition, temperature, and degree of departure from equilibrium conditions. These characteristics typically vary substantially throughout the flowfield, so radiative properties cannot be represented accurately with simple models, but rather call for modeling at the molecular or atomic level (Jaffe et al., 2014). Johnston, et al (2013) note the dearth of molecular data for doing so, and uncertainties as high as 100% in many cases. Brandis, et al (2013) report better agreement (within 46%) between computation and experimental data from shock tube tests, but point out the uncertainty associated with nonequilibrium in interpreting the data.

Currently, there are three leading computational tools capable of modeling at the molecular level to appropriately predict radiative transport in the shock and boundary layer during re-entry: NEQAIR, HARA, and HyperRad (Jaffe et al. 2014). The oldest of the three, developed in the mid-90s, Nonequilibrium Air Radiation (NEQAIR) (Whiting et al. 1996) is a line by line radiation code used to compute spontaneous emission, stimulated emission, and absorption due to transitions between different energy states (Brandis et al. 2013). Similarly, Hypersonic Air Radiation Algorithm (HARA) is a radiation code that applies up-to-date spectral and excitation rate data to an efficient algorithm (Johnston et al. 2013). It Its purpose is the simulation of high-energy

hypersonic flow (Wood, 2012). A most recent code, HyperRad, is currently being developed at NASA Ames Research Center. It is meant for incorporation into hypersonic flow codes and includes line spectra based on *ab initio* calculation from quantum physics (Howell et al. 2010).

These computation efforts have been undertaken in an effort to expand and update the spectral databases available from NIST (Ralchenko, 2006), primarily, via *ab initio* computation of atomic or molecular energy or "Einstein Coefficients". NEQAIR and HARA codes have been compared and they do produce very similar spectra. However, HyperRad is not compared against NEQAIR and HARA because it uses its own database (Brandis et al. 2013).

From a recent National Aeronautics and Space Administration (NASA) Early Career Faculty (ECF) solicitation (NNH15ZOA001N-15ECF-B1), "The current state of the art for predicting aerothermal environments for planetary entry are dependent on physical models and underlying numerical methods that are, in many cases, two to five decades old." The solicitation sought, "innovative physical models for high-speed non-equilibrium flows (such as state-specific models to reduce predictive uncertainty for non-equilibrium radiation)," and, "novel approaches to obtain validation data for these models (such as calibrated spectroscopic experiments in a shock tube or plasma facility or rapid ab initio calculations)". Due to this solicitation, this work is done in order to update the numerical methods that are old by using the rapid ab initio calculations.

"State-specific" here refers to release or absorption of a photon of radiation at a particular frequency via a molecular energy transition. The first principles of the known physics relevant to this problem are embodied in the "quantum mechanical" description

of molecular energies. The first step of such an *ab initio* implementation is integration of the time independent Schrödinger's equation for the lower and upper molecular energy levels of a transition. Schrödinger's wave equation is a Sturm-Liouville eigenvalue differential equation. Analytical solutions exist for only a few simple cases. In general, numerical methods must be used.

Some popular computational methods employing the three-dimensional Schrödinger's equation used to date are shooting methods (Numerov's method), matrix methods, finite element method (FEM), and variational Rayleigh - Ritz - Galerkin methods.

The shooting method (Numerov's method) is a finite difference method used to solve a boundary value problem (BVP) by reducing it to an initial value problem. The method considers the boundary conditions as a multivariate function of initial condition at some point and reduces it to obtain the initial condition which provides a root. Advantages of this method are speed and adaptability, however it lacks robustness. The matrix method involves expressing the equation in the form of a matrix using finite differences. The finite element method finds an approximate solution to a boundary value problem by subdividing a large problem into smaller, simpler parts, called finite elements. The simple equations that model the finite elements are then assembled into a larger equation that model the entire problem. Lastly, the variational Rayleigh-Ritz-Galerkin method is a direct method to solve a boundary value problem by finding its approximate solution. It is a special case of FEM as the process is to convert a continuous operator problem to a discrete problem.

Any of these four computational methods can provide accurate solutions to the

three-dimensional Schrödinger's equation, however the shooting, FEM, and variational Rayleigh - Ritz - Galerkin method need to have a good initial guess to the eigenfunctions as well as eigenvalues, while the matrix method is a more global approach. In addition, no iterations, matching and relaxation are needed (Salejda et al. 2000). Although the matrix method is the most global approach to computing the three-dimensional Schrödinger's equation, the most popular method to integrate Schrödinger's equation to date is the shooting method (Numerov's method) due to the simplistic final form of equation. However, this equation may only be used to calculate the wave function of the hydrogen atom or hydrogen-like atom. Slight variations of the equation will be needed to calculate the other atoms.

Even though the matrix method is a more global approach, only a few researchers have made the attempts to use this approach (Salejda et al and Van der Maelen Uria et al). Salejda et al (2000) have successfully built a program that is able to compute eigenvalues and eigenfunctions using the matrix method, but used Dirichlet boundary conditions, which are not correct for all cases. Van der Maelen Uria et al (1995) uses the QR algorithm to solve the matrix equation and also uses Dirichlet boundary conditions. The QR algorithm in numerical linear algebra is an eigenvalue algorithm, which is a procedure that used to calculate the eigenvalues and eigenvectors of a matrix. The idea is to write a matrix as a product of an orthogonal matrix and an upper triangular matrix, which then used to multiply the factor in the reverse order and iterate. However, this method may only compute both eigenvalue and eigenvector if the original matrix is symmetric. If the original matrix is not symmetric, only eigenvalues will be computed. These attempts were used to solve a one-dimensional Schrödinger's equation. We have

not yet found an attempt to solve a two-dimensional or three-dimensional Schrödinger's equation by the matrix method.

For a three-dimensional case, Khelashvili et al. (n.d.) suggested the radial equation obeys the Dirichlet boundary condition and Brazier-Smith (1983) suggested that the spherical harmonics, which are discussed in section 4.2, obey the Dirichlet and Von Neumann boundary conditions. Both authors used Numerov's method to numerically compute the three-dimensional Schrödinger's equation. However, these boundary conditions do not yield the correct results when the matrix method is used, but only for some particular results known analytically.

## 1.2. Problem Statement

The objective is to develop the matrix method in such a way as to be extendable to general molecular species. The approach is to cast the Schrödinger wave equation as a matrix eigenvalue problem, using finite differences for the derivatives. The equation can be solved using the ERAU parallel supercomputer, on which resides the LAPACK numerical library for linear systems. The proposed work will focus on the hydrogen atom because analytical solutions are available with which to verify the numerical results.

Perhaps the largest challenge is to develop general boundary conditions sans a priori knowledge of the solution. One does not wish to restrict the "solution space." Even given analytical solutions for the hydrogen atom, certain known boundary conditions, e.g. zero Dirichlet, do not apply for all cases. The matrix method will yield all solutions that can be "captured" by the chosen grid refinement, and consistent with the boundary formulation.

The resulting eigenvalues are the allowable energy levels, and the eigenvectors a discrete "data table" representation of the wave functions versus spatial coordinates of the molecular particles. Numerically integrating wave functions for two energy levels with the dipole moment of the transition between them, yields the Einstein coefficients – molecular properties that give rates of transition, hence rates of absorption or emission of photons of radiation. It should be noted that a large molecule may contain thousands of energy states, hence tens of thousands of Einstein coefficients.

Computing emissivities and absorptivities for particular transitions – that is, state- or wavelength-specific – is then straightforward. The complete procedure is potentially much more efficient and comprehensive than experimental studies.

## 2. Theory and Governing Equations

### 2.1. Classical Macroscopic Description

In order to fully understand heat transfer due to radiation, Beer's law is considered. Beer's law states that the decrease in the intensity of the radiation $I$, which has units of erg s$^{-1}$ cm$^{-2}$ sr$^{-1}$, passing through a layer of thickness $dx$, is proportional to the intensity of the radiation and its thickness.

$$dI(x) = -\kappa_R I(x) dx$$

(2.1)

Here $\kappa_R$ is the absorption (or extinction) coefficient which is a measure of the rate of decrease in the intensity of electromagnetic radiation. Integrating equation 2.1 with constant absorption coefficient gives the exponential decal law form for the decrease in intensity.

The Fourier form, a conduction heat transfer analog, is sometimes simpler to implement. Let the differential fluid element have area $dA$. The incoming heat flux is defined as $q$ (erg s$^{-1}$ cm$^{-2}$) and the outgoing heat flux as $q - dq$. The difference yields the rate of energy increase within the fluid element as

$$dq dA = \rho C_v \frac{dT}{dt} dA dx$$

(2.2)

where $\frac{dT}{dt} = \frac{dT}{dx} c_0$. Therefore equation 2.2 can be re-written as

$$\frac{dq}{dx} = \rho C_v c_0 \frac{dT}{dx}$$

(2.3)

As the radiation heat flux is the same quantity as intensity $I$, equation 2.1 and 2.3 can be rewritten as

$$\rho C_v c_0 \frac{dT}{dx} = \frac{dI}{dx} = -\kappa_R I = -\kappa_R q \tag{2.4}$$

By using equation 2.4, radiative heat flux can be determined.

$$q = -\frac{\rho C_v c_0}{\kappa_R} \frac{dT}{dx} \tag{2.5}$$

From Fourier's law,

$$q = -\beta_R \frac{dT}{dx} \tag{2.6}$$

where $\beta_R$ is the "radiative thermal conductivity." Comparing equation 2.6 to equation 2.5,

$$\beta_R = \frac{\rho C_v c_0}{\kappa_R} \tag{2.7}$$

## 2.2. Quantum Mechanical Description

Absorption coefficients have typically been measured experimentally in the past. Experimentation is difficult for gases at re-entry temperatures. Absorption coefficients can be computed via quantum mechanics however. Their frequency dependencies can be computed as well.[1]

Thermal radiation results from a change in atomic and molecular energy levels resulting from spontaneous and stimulated transitions. These transitions, in a bounded quantum mechanical system, can take on only certain discrete values of energy. In other words, energy levels of electrons in atoms, ions, or molecules are quantized. Lower, more

---

[1] We have not addressed this in the previous section, but will in what follows.

populous energy levels are said to be in the ground state, while higher energy levels are referred to as excited states.

A photon of radiation energy is emitted or absorbed when the electronic level falls from an upper to lower level, or is raised from a lower to an upper level, respectively. As depicted in Figure 1, there exist three processes by which electron transitions occur: spontaneous emission, absorption, and stimulated emission.
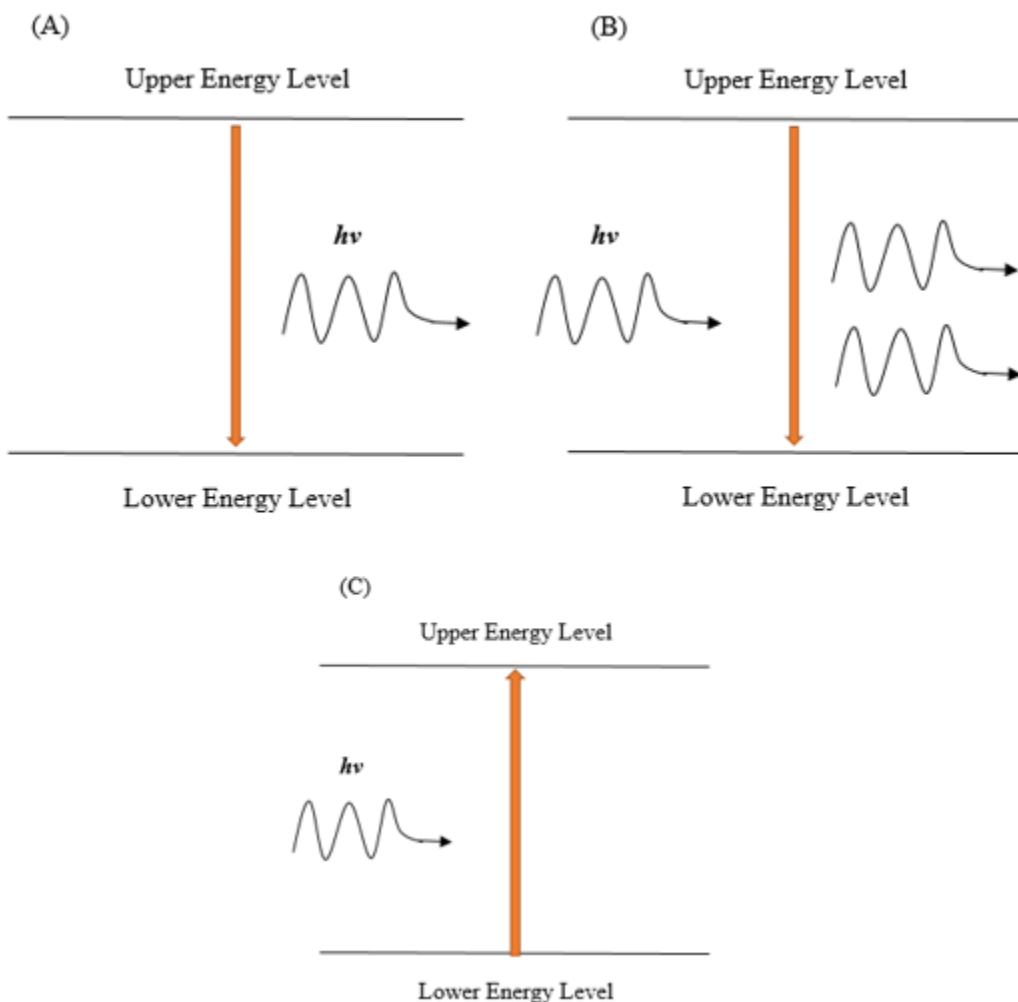


Figure 2.1. (A) Spontaneous emission, (B) Stimulated emission, and (C) Absorption

Figure 2.1 (A) illustrates spontaneous emission, when an atom falls to a lower

energy level and emits of a photon in the absence of external radiation. These upper to lower level transitions occur at rates specific to each atomic species and its electronic energy levels. The rates are called "Einstein A coefficients" and are usually given the symbol $A_{UL}$ $(s^{-1})$. The A coefficient is the rate per atom at which energy level $U$ falls to level $L$, emitting a photon.

Stimulated emission, Figure 2.1 (B), occurs when a photon passes an atom and temporarily raises its energy from a lower to an upper level, which then returns to the lower level. This rate is also called the "Einstein B coefficient for stimulated emission," and is usually given by the symbol $B_{UL}$. Units of $B_{UL}$ are discussed below.

Absorption, as shown in Figure 2.1 (C), occurs when a photon strikes an atom and raises its energy from a lower to an upper level. This rate is called the "Einstein B coefficient for absorption" and is usually given the symbol $B_{LU}$ with the same units as $B_{UL}$.

It is important to note that the A and B coefficients are constant physical properties of a substance, as postulated by Einstein (Einstein, A., 1917). They have no dependency on temperature or other variables.

The energy of an emitted or absorbed photon of radiation can be calculated by taking the difference between the energy levels as

$$E_U - E_L = h\nu \tag{2.8}$$

where $h = 6.625 \times 10^{27}$ erg s is Planck's constant, and $\nu$ is the frequency in s$^{-1}$.

Now the rate of depopulation of an upper level $U$ to a lower level $L$ by spontaneous emission is

$$\left.\frac{dn_u}{dt}\right|_{UL} = -n_U A_{UL} \tag{2.10}$$

where $n_U$ is the number density of atoms at the upper level.

The rate of population increase of the upper energy level from the lower due to absorption is shown in equation 2.11.

$$\left.\frac{dn_u}{dt}\right|_{LU} = n_L B_{LU} \int_0^{4\pi} I_v(\Omega) d\Omega \tag{2.11}$$

$I_v$ is the derivative of the intensity with respect to the frequency and is called the spectral intensity (erg s$^{-1}$ cm$^{-2}$ sr$^{-1}$ Hz$^{-1}$). We use Hz to denote the units of the spectral variable, frequency. The directional dependency of the intensity, indicated by the $\Omega$ functionality, and by sr$^{-1}$, is integrated over $4\pi$ steradians. $B_{LU}$ has units of frequency times area per erg (Hz cm$^2$ erg$^{-1}$).

Lastly, the rate of change of an electron from upper energy level to a lower energy level by stimulated emission is shown in equation 2.12. Upper to lower level transitions result from the presence of photons of the same frequency as the transition.

$$\left.\frac{dn_u}{dt}\right|_{UL} = n_L B_{UL} \int I_V d\Omega \tag{2.12}$$

From Planck's law, the Einstein A Coefficient and Einstein B Coefficients are related by equation 2.13 (Vincenti and Kruger, 1965).

$$A_{UL} = \frac{8\pi h v^3}{c^2} B_{UL} \tag{2.13}$$

$$g_U B_{UL} = g_L B_{LU} \tag{2.14}$$

$g_U$ and $g_L$ shown in equation 2.14 are the molecular degeneracies of the upper energy level and lower energy level, respectively. The molecular degeneracy is the number of ways in which electrons are able to exist at a discrete energy level. From equation 2.14, the absorption and stimulated emission can then be considered by following the rate of change of the population that can be defined as

$$\frac{dn_u}{dt} = (n_L B_{LU} - n_U B_{UL}) \int_0^{4\pi} I_v \; d\Omega \tag{2.15}$$

Through restricting the intensity into a single direction, equation 2.15 can be rewritten as

$$\frac{d}{d\Omega} \frac{dn_U}{dt} = (n_L B_{LU} - n_U B_{UL}) I_v \tag{2.16}$$

The left hand side of equation 2.16 is the rate at which the transitions occur from the lower to upper energy level per volume in a particular direction, with units of $s^{-1} cm^{-3} sr^{-1}$. As the transition that occur from the lower to upper energy levels removes a photon $hv$, equation 2.16 can be rewritten into equation 2.17 which has units of $erg\ s^{-1} cm^{-3} sr^{-1}$.

$$hv \frac{d}{d\Omega} \frac{dn_U}{dt} = hv \, (n_L B_{LU} - n_U B_{UL}) I_{v_0} \tag{2.17}$$

Equation 2.17 is the rate of absorption of incident intensity at frequency $\nu$ per unit depth in the $\Omega$ direction.

A subtle point that must be made here is that $I_\nu$ as we have defined it is a probability distribution of intensity over frequency, due to various "line broadening" effects which we will not discuss here. In the above equation we have identified a single frequency associated with a particular *UL* transition, so that we have effectively integrated $I_\nu d\nu$ over the "line width" as $\nu I_{\nu 0}$, where $I_{\nu 0}$ is some suitable average value.

Clearly the left hand side then is just $\nu \dfrac{dI_{\nu_0}}{dx}$, so that finally

$$\frac{dI_{\nu_0}}{dx} = -h\left(n_L B_{LU} - n_U B_{UL}\right)I_{\nu_0}$$

(2.18)

Comparing with equation (2.1), we can define a spectral absorption coefficient as

$$KR_\nu = h(n_L B_{LU} - n_U B_{UL})$$

(2.19)

Now the Einstein *B* coefficient can be computed as (Atkins et al, 2011),

$$B_{LU} = \frac{|\mu_{UL}|^2}{6\varepsilon_0 \hbar^2}$$

(2.20)

where $\mu_{UL}$ denotes the transition dipole moment. The transition dipole moment is a measure of energy an electron can deliver to the electromagnetic field during the transition. It depends upon the probabilities of its existence at level *U*, and at level *L*.

In 1926, an American physicist Erwin Schrödinger formulated an equation based on the conservation of energy using "quantum operators" and the de Broglie relations which describe the wave properties of microscopic particles (Schrödinger, 1926). Schrödinger's equation is a Sturm-Liouville eigenvalue partial different equation whose solutions exist for only discrete values of the particle energy. The energies are the

eigenvalues, and the "wave functions" that solve the equation are the eigenfunctions. In Born's statistical interpretation, the squared modulus of the wave function is a real number and can be interpreted as the probability density of a particle being detected at a given place or time. For present purposes we can restrict our attention to the time-independent form of Schrödinger's equation.

$$-\frac{\eta^2}{2m}\nabla^2\Psi(\vec{x})+V(\vec{x})\Psi(\vec{x})=E\Psi(\vec{x})$$

(2.21)

Here $\eta$ (h bar) is Planck's constant divided by $2\pi$, $m$ is the particle mass (an electron in our problem), $\Psi$ is the wave function, $V$ a potential energy, $E$ the energy eigenvalue, and $\vec{x}=(x,y,z)$ the spatial domain.

From the solutions for the wave functions of energy levels $U$ and $L$ we can compute the transition dipole moment from

$$\mu_{UL}=\int\psi_U^*\mu\psi_L d\tau$$

(2.22)

Here, $\psi_U^*$ is the wave function on the upper level, $\psi_L$ is the wave function on the lower level, the electric dipole operator $\mu$ is the charge on the electron times its distance from the nucleus, and it has units of Coulomb times length (C cm).

### 3. Application to the Hydrogen Atom

### 3.1. Schrödinger's Equation in 3D Spherical Coordinate System

In order to model the hydrogen atom, it is necessary to formulate the Hamiltonian in three dimensions and it is appropriate to formulate it in spherical polar coordinates $(r, \theta, \phi)$ which is shown in Figure 2, where $r$ indicates the distance from the origin to the surface, $\theta$ indicates the angle of the radial vector measured from the positive z-axis, and $\phi$ indicates the angle measured counterclockwise from the positive x-axis when viewed from above. The solution from Schrödinger's equation will give the probability of finding an electron at a particular position relative to the nucleus, which is located at the origin $(O)$ of the graph.
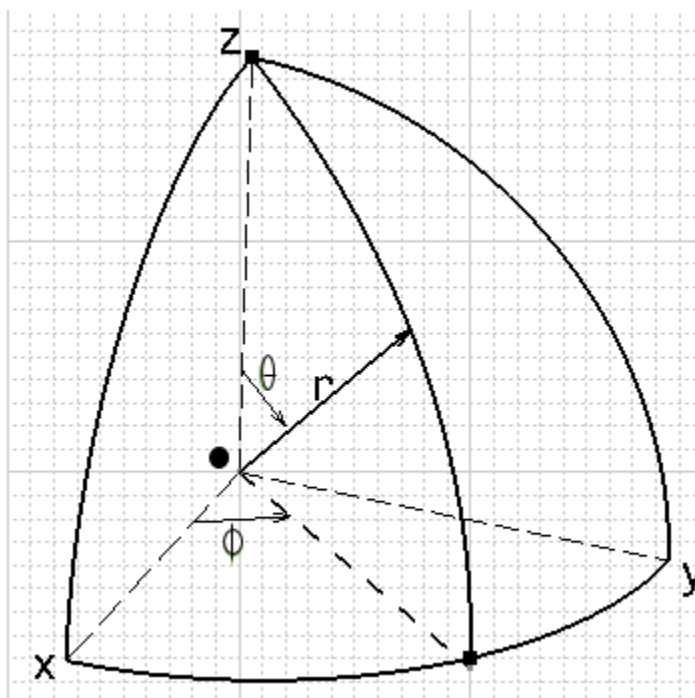


Figure 3.1. Spherical Coordinates in Three-Dimensional

Equation 3.1 below shows the Schrödinger's equation in spherical coordinates

$$\left\{\frac{-\hbar^2}{2m}\left[\frac{1}{r}\frac{\partial^2}{\partial r^2}r + \frac{1}{r^2}\frac{1}{\sin^2\theta}\frac{\partial^2}{\partial\phi^2} + \frac{1}{r^2}\frac{1}{\sin\theta}\frac{\partial}{\partial\theta}\sin\theta\frac{\partial}{\partial\theta}\right]\right.$$
$$\left. + V(r)\right\}\Psi(r,\theta,\phi) = E\psi(r,\theta,\phi)$$

(3.1)

Note that the potential $(V)$ is a function of $r$ as this equation is for hydrogen atom case, which will be explained more in section 4.3.

## 3.2. Separation of Variables

From subsequent solutions for Hydrogen atom or Hydrogen-like atom, it is assumed that the variables are separable.

$$\Psi(r,\theta,\phi) = R(r)\,Y(\theta,\phi)$$

(3.2)

where

$$Y(\theta,\phi) = \Phi(\phi)\Theta(\theta)$$

(3.3)

Using equation 3.3 and dividing it with $\frac{-\hbar^2}{2mr^2}$, equation 3.1 can be simplified to

$$\left[r\frac{\partial^2}{\partial r^2}r + \frac{1}{\sin^2\theta}\frac{\partial^2}{\partial\phi^2} + \left(\frac{1}{\sin\theta}\frac{\partial}{\partial\theta}\right)\left(\sin\theta\frac{\partial}{\partial\theta}\right) + V(r)\right]R(r)\,Y(\theta,\phi)$$

(3.4)

$$= -\frac{E\,2mr^2}{\hbar^2}R(r)\,Y(\theta,\phi)$$

Focusing on the equation on the left hand side and defining the moment of inertia as, $I = mr^2$, equation 3.4 can be simplified to

$$\left[ rY\{rR'' + R'\} + R\frac{1}{sin^2\theta}\frac{\partial^2 Y}{\partial\phi^2} + \left(R\frac{1}{sin\,\theta}\frac{\partial}{\partial\theta}\right)\left(sin\,\theta\frac{\partial Y}{\partial\theta}\right) + V(r) \right] \tag{3.5}$$

$$= -\frac{2EI}{\hbar^2}R\,Y$$

Dividing equation 3.5 with $R(r)Y(\theta,\phi)$,

$$\left[ \frac{r}{R}\{rR'' + R'\} + \frac{1}{Y}\frac{1}{sin^2\theta}\frac{\partial^2 Y}{\partial\phi^2} + \frac{1}{Y}\left(\frac{1}{sin\,\theta}\frac{\partial}{\partial\theta}\right)\left(sin\,\theta\frac{\partial Y}{\partial\theta}\right) + V(r) \right] \tag{3.6}$$

$$= -\frac{2EI^2}{\hbar^2}$$

Setting $k = \frac{2EI}{\hbar^2}$ and note that $k$ is a function of $r$ only,

$$\left[ rY\{rR'' + R'\} + R\frac{1}{sin^2\theta}\frac{\partial^2 Y}{\partial\phi^2} + \left(R\frac{1}{sin\,\theta}\frac{\partial}{\partial\theta}\right)\left(Y\,sin\,\theta\frac{\partial}{\partial\theta}\right) + V(r) \right] \tag{3.7}$$

$$+ k = 0$$

Separating $R$ and $Y$ from equation 3.7,

$$\frac{r}{R}\{r\,R'' + R'\} + V(r) + k = \lambda \tag{3.8}$$

$$\frac{1}{Y}\frac{1}{sin^2\theta}\frac{\partial^2 Y}{\partial\phi^2} + \frac{1}{Y}\frac{1}{sin\theta}\frac{\partial}{\partial\theta}sin\,\theta\frac{\partial Y}{\partial\theta} = -\lambda \tag{3.9}$$

Substituting equation 3.3 to equation 3.9, and by using the separation of variables,

$$\left[ \frac{1}{sin^2\theta}\frac{\partial^2}{\partial\phi^2} + \frac{1}{sin\theta}\frac{\partial}{\partial\theta}sin\,\theta\frac{\partial}{\partial\theta} \right]\Phi(\phi)\Theta(\theta) = -\lambda\Phi(\phi)\Theta(\theta) \tag{3.10}$$

$$\frac{\Theta(\theta)}{sin^2\theta}\frac{\partial^2\Phi}{\partial\phi^2} + \frac{\Phi(\phi)}{sin\,\theta}\frac{\partial}{\partial\theta}sin\,\theta\frac{\partial\Theta}{\partial\theta} = -\lambda\Phi(\phi)\Theta(\theta) \tag{3.11}$$

$$\frac{1}{\Phi(\phi)}\frac{\partial^2\Phi}{\partial\phi^2} + \frac{1}{\Theta(\theta)}sin\,\theta\frac{\partial}{\partial\theta}sin\,\theta\frac{\partial\Theta}{\partial\theta} = -\lambda\,sin^2\theta \tag{3.12}$$

$$\frac{1}{\Phi(\phi)}\frac{\partial^2 \Phi}{\partial \phi^2} = -m_l{}^2 \tag{3.13}$$

$$\lambda \, sin^2\theta + \frac{1}{\Theta(\theta)} \, sin \, \theta \, \frac{\partial}{\partial \theta} \, sin \, \theta \, \frac{\partial \Theta}{\partial \theta} = m_l{}^2 \tag{3.14}$$

Equations (3.8), (3.14), and (3.13) are the separated wave equations for $R(r)$, $\Theta(\theta)$, and $\Phi(\phi)$, respectively. Two separation constants have been introduced, $\lambda$ and $m_l^2$.

# 4. Analytical Solutions for the Hydrogen Atom

## 4.1. Particle on a Ring – the Phi Equation

The simplest of these is equation (3.13).  In the literature this is often called the, "particle on a ring" problem. Its general solution is

$$\Phi = Ae^{im_l\phi} + Be^{-im_l\phi}$$

(4.1)

$m_l$ is a dimensionless number. As the wave function depends only on the angle $\phi$, boundary conditions can be introduced. A cyclic boundary condition shown in equation (4.2) is used, since there are no barriers to the particle's motion as long as it moves on the ring (Levine, 2014). Hence, there is no requirement for the wave function to vanish at any point on the ring.

$$\Phi(\phi + 2\pi) = \Phi(\phi)$$

(4.2)

$$A\exp(im_l\phi) + B\exp(-im_l\phi) = A\exp(im_l\phi)\exp(2\pi im_l)$$
$$+ B\exp(-im_l\phi)\exp(-2\pi im_l)$$

(4.3)

It follows that,

$$e^{2\pi m_l\phi} = e^{-2\pi m_l\phi} = 1 \qquad m_l = 0, \pm 1, \pm 2, \pm 3, \dots$$

(4.4)

To normalize the wave function (equation 4.1), each term is expanded according to Euler's relation.

$$\Phi = A[\cos(m_l\phi) + i\,\sin(m_l\phi)] + B[cos(m_l\phi) - i\,sin(m_l\phi)] \tag{4.5}$$

$$\Phi = (A + B)\cos(m_l\phi) + (A - B)\,i\,\sin(m_l\phi) \tag{4.6}$$

$$\Phi^* = (A + B)\,cos(m_l\phi) - (A - B)\,i\,sin(m_l\phi) \tag{4.7}$$

By multiplying equation 4.5 and equation 4.6 together,

$$\Phi\,\Phi^* = (A^2 + B^2)[cos^2(m_l\phi) + sin^2(m_l\phi)] \\ + 2AB[cos^2(m_l\phi) - sin^2(m_l\phi)] \tag{4.8}$$

$$\Phi\,\Phi^* = (A^2 + B^2) + 2AB[cos^2(m_l\phi) - sin^2(m_l\phi)] \tag{4.9}$$

By looking at Figure 4 from the section "Schrodinger equations in spherical coordinates", it can be seen that the particle only moves from $(0 - 2\pi)$. This domain is used to integrate and simplify equation 4.10 as follows

$$A^2 + B^2 = \frac{1}{2\pi} \tag{4.10}$$

The sign of the eigenvalue determines the direction of travel of the particle so either $A = 0$ or $B = 0$. Equation (4.1) can be written as,

$$\Phi(\phi) = \frac{1}{\sqrt{2\pi}}e^{im_l\phi} \qquad\qquad m_l = 0, \pm1, \pm2, \pm3, \ldots \tag{4.11}$$

## 4.2. Particle on a Sphere – the Theta Equation

Classical solution for particle on a sphere can found in a number of textbooks. This follows that of Atkins et al. Equation (3.14) from the section "Schrödinger's

Equation in Spherical Coordinates" denotes a particle on a sphere. From (3,14)

$$\frac{1}{\sin\theta}\frac{\partial}{\partial\theta}\sin\theta\frac{\partial\Theta}{\partial\theta} - \frac{m_l{}^2\Theta}{\sin^2\theta} + \lambda\Theta = 0 \tag{4.12}$$

Introducing a variable substitution,

$$z = \cos\theta \tag{4.13}$$

$$\frac{\partial z}{\partial\theta} = -\sin\theta \tag{4.14}$$

$$\frac{\partial}{\partial\theta} = \frac{\partial}{\partial z}\frac{\partial}{\partial\theta} = -\frac{\partial}{\partial z}\sin\theta \tag{4.15}$$

Defining

$$P(z) = \Theta(\theta) \tag{4.16}$$

Equation (4.12) is transformed to

$$\frac{-1}{\sin\theta}\frac{\partial}{\partial\theta}\sin^2\theta\frac{\partial P}{\partial z} - \frac{m_l{}^2\Theta}{\sin^2\theta} + \lambda\Theta = 0 \tag{4.17}$$

Using trigonometric substitution

$$\sin^2\theta = 1 - z^2 \tag{4.18}$$

Equation (4.17) can be simplified to

$$-\frac{1}{\sin\theta}\frac{\partial}{\partial\theta}(1-z^2)\frac{\partial P}{\partial z} - \frac{m_l{}^2\Theta}{(1-z^2)} + \lambda\Theta = 0 \tag{4.19}$$

Applying chain rule to equation (4.19),

$$\frac{\partial}{\partial z}\left[(1-z^2)\frac{\partial P}{\partial z}\right] + \left[\lambda - \frac{m_l{}^2}{(1-z^2)}\right]P = 0 \tag{4.20}$$

Defining

$$P(z) = \left(1 - z^2\right)^{|m_l|/2} G(z) \tag{4.21}$$

$$P'(z) = \left(1 - z^2\right)^{|m_l|/2}\left[G' - \frac{|m_l|z}{\left(1 - z^2\right)}G(z)\right] \tag{4.22}$$

$P(z)$ can be identified as the associated Legendre functions. Using equation (4.21) and (4.22), equation (4.20) becomes,

$$
\begin{aligned}
&\frac{\partial}{\partial z}\left[\left(1 - z^2\right)\frac{\partial P}{\partial z}\right] + \left[\lambda - \frac{m_\lambda^2}{1 - z^2}\right]P \equiv \\
&\left(1 - z^2\right)^{|m_\lambda|/2 + 1}\left[G'' - \frac{\left(1 - z^2\right)|m_\lambda|(zG' + G) - 2|m_\lambda|z^2 G}{\left(1 - z^2\right)^2}\right] \\
&- 2z\left(\frac{|m_\lambda|}{2} + 1\right)\left(1 - z^2\right)^{|m_\lambda|/2}\left[G' - \frac{|m_\lambda|zG}{1 - z^2}\right] \\
&+ \left[\lambda - \frac{m_\lambda^2}{1 - z^2}\right]\left(1 - z^2\right)^{|m_\lambda|/2} G
\end{aligned} \tag{4.23}
$$

Dividing equation 4.25 with $\left(1 - z^2\right)^{|m_\lambda|/2}$ and rearranging,

$$
\begin{aligned}
&\left(1 - z^2\right)G'' + \left[-|m_\lambda|z - 2\left(\frac{|m_\lambda|}{2} + 1\right)z\right]G' \\
&+ \left[-|m_\lambda| - \frac{2|m_\lambda|z^2}{1 - z^2} + 2\left(\frac{|m_\lambda|}{2} + 1\right)\frac{|m_\lambda|z^2}{1 - z^2} + \lambda - \frac{m_\lambda^2}{1 - z^2}\right]G = 0
\end{aligned} \tag{4.24}
$$

By simplifying equation 4.26,

$$(1 - z^2)G'' - 2z(1 + |m_l|)G' + (\lambda - |m_l| - m_l{}^2)G = 0 \tag{4.25}$$

Assuming $G$ a polynomial,

$$G(z) = \sum_{n=0}^{\infty} a_n z^n \tag{4.26}$$

$$G'(z) = \sum_{n=1}^{\infty} n a_n z^{n-1} = \sum_{n=0}^{\infty} n a_n z^{n-1} = \sum_{n=0}^{\infty} (n+1) a_{n+1} z^n \tag{4.27}$$

$$G''(z) = \sum_{n=2}^{\infty} n(n-1) a_n z^{n-2} = \sum_{n=0}^{\infty} n(n-1) a_n z^{n-2} \tag{4.28}$$

$$= \sum_{n=0}^{\infty} (n+1)(n+2) a_{n+2} z^n$$

Substituting equation (4.26), (4.27), and (4.28) to equation (4.25),

$$\sum_{n=0}^{\infty} \{(1-z^2)n(n-1)a_n z^{n-2} - 2z(1+|m_l|)n a_n z^{n-1} \tag{4.29}$$

$$+ (\lambda - m_l^2 - |m_l|)a_n z^n\} = 0$$

The first term in equation (4.29), $(1-z^2)n(n-1)a_n z^{n-2}$ can be written as,

$$\sum_{n=0}^{\infty} \{(n+2)(n+1)a_{n+2}z^n - n(n-1)a_n z^n\} \tag{4.30}$$

Substitute equation (4.30) to equation (4.29),

$$\sum_{n=0}^{\infty} z^n\{(n+2)(n+1)a_{n+2} - n(n+1)a_n - 2(1+|m_l|)n a_n \tag{4.31}$$

$$+ (\lambda - m_l^2 - |m_l|)a_n\} = 0$$

When $z = \cos\theta = 1$, the series diverges unless it terminates for some value of $n$.

So for some value of $n$,

$$(n+2)(n+1)a_{n+2} = \left[n(n-1) + 2(1+|m_\lambda|)n - (\lambda - m_\lambda^2 - |m_\lambda|)\right]a_n \tag{4.32}$$

Equation (4.32) then can be simplified to

$$a_{n+2} = \frac{(n+|m_l|)(n+|m_l|+1) - \lambda}{(n+1)(n+2)} a_n \tag{4.33}$$

Therefore,

$$\lambda = (n + |m_l|)(n + |m_l| + 1)$$
(4.34)

$$\lambda = l(l+1)$$
(4.35)

$$l = n + |m_l| \qquad n = 0,1,2, \dots$$
(4.36)

$\Theta(\theta)$ can be constructed as

$$\Theta(\theta) = sin^{|m_l|}\theta \sum_{\substack{n=0,2,4 \\ n=1,3,5}}^{l-|m_l|} a_n cos^n \theta$$
(4.37)

The specific relation between the normalized function and the associated Legendre function is

$$\Theta(\theta) = \left\{ \left( \frac{2l+1}{2} \right) \frac{(l-|m_l|)!}{(l+|m_l|)!} \right\}^{\frac{1}{2}} P_l^{|m_l|}(\cos\theta)$$
(4.38)

Using normalization condition, $a_0$ coefficient can be determined

$$\int_0^\pi \Theta^2(\theta) \sin\theta \, d\theta = 1$$
(4.39)

Substituting equation (4.37) to equation (4.39) and by calculating $\Theta(\theta)$ for $m_l = 0,1,2, \dots$ and $l = 0,1,2, ..$ the analytical solution of $\Theta(\theta)$ equation can be found. Table 4.1 shows a few of the analytical eigenfunctions.

Table 4.1 Analytical Results of $\Theta(\theta)$

| Analytical Eigenfunctions | | |
|---|---|---|
| $l$ | $m_l$ | $\Theta(\theta)$ |
| 0 | 0 | $\dfrac{\sqrt{2}}{2}$ |
| 1 | 0 | $\dfrac{\sqrt{6}}{2}\cos\theta$ |
| | $\pm 1$ | $\dfrac{\sqrt{3}}{2}\sin\theta$ |
| 2 | 0 | $\dfrac{\sqrt{10}}{4}(3cos^2\theta - 1)$ |
| | $\pm 1$ | $\dfrac{\sqrt{15}}{2}\sin\theta\cos\theta$ |
| | $\pm 2$ | $\dfrac{\sqrt{15}}{4}sin^2\theta$ |
| 3 | 0 | $\dfrac{3\sqrt{14}}{4}\left(\dfrac{5}{3}cos^3\theta - \cos\theta\right)$ |
| | $\pm 1$ | $\dfrac{\sqrt{42}}{8}\sin\theta\,(5cos^2\theta - 1)$ |
| | $\pm 2$ | $\dfrac{\sqrt{105}}{4}sin^2\theta\cos\theta$ |
| | $\pm 3$ | $\dfrac{\sqrt{70}}{8}sin^3\theta$ |

### 4.3. The Radial Equation

The potential energy in the radial equation, (3.8) is the Coulombic potential.

$$V(r) = -\frac{Ze^2}{4\pi\epsilon_0 r} \tag{4.40}$$

where $Z$ is the atomic number, which for the hydrogen atom will be 1. $\epsilon_0$ is the quantity

of vacuum permittivity which has a value of $8.854 \times 10^{-12}$ C² N⁻¹ m⁻².

Substituting $k, \lambda, I$, and (4.40) into equation 3.8 and rearranging,

$$-\frac{\hbar^2}{2m}\left\{R'' + \frac{2}{r}R'\right\} + \frac{l(l+1)\hbar^2 R}{2mr^2} - \frac{Ze^2}{4\pi\epsilon_0 r}R = ER \tag{4.41}$$

Using an operator notation in order to define a function of the differentiation

operator ($R'' = \frac{\partial^2}{\partial r^2}$ and $R' = \frac{\partial}{\partial r}$), equation 4.41 can be re-written as

$$-\frac{\hbar^2}{2m}\left\{\frac{\partial^2}{\partial r^2} + \frac{2}{r}\frac{\partial}{\partial r}\right\} + \left[\frac{l(l+1)\hbar^2}{2mr^2} - \frac{Ze^2}{4\pi\epsilon_0 r}\right]R = ER \tag{4.42}$$

Solutions of the radial wave equation can be found in many different textbooks.

According to (Atkins et al, 2011) and (Abramowits et al, 1965), the acceptable solutions

for radial wave function are the associated Laguerre functions. By incorporating the

associated Laguerre functions into radial wavefunction, the analytical solutions for few

lower orbitals can be shown in Table 2.

$$R_{nl}(r) = -\left\{\left(\frac{2Z}{na}\right)^3 \frac{(n-l-1)!}{2n[(n+l)!]^3}\right\}\rho^l L_{n+l}^{2l+1}(\rho)e^{-\frac{\rho}{2}} \tag{4.43}$$

Where $\rho = \left(\frac{2Z}{na}\right)r$ and $a = \frac{4\pi\varepsilon_0\hbar^2}{\mu e^2}$ is the Bohr radius which has a value of

$5.529576 \times 10^{-9}$ cm.

Table 4.2 Radial Wave Functions

| $n$ | $l$ | $R_{nl}(r)$ |
|---|---|---|
| 1 | 0 | $2\left(\dfrac{Z}{a}\right)^{\frac{3}{2}} e^{-\frac{Zr}{a}}$ |
| 0 | 2 | $\dfrac{1}{\sqrt{2}}\left(\dfrac{Z}{a}\right)^{\frac{3}{2}}\left(1-\dfrac{Zr}{2a}\right) e^{-\frac{Zr}{2a}}$ |
| 1 | 2 | $\dfrac{1}{2\sqrt{6}}\left(\dfrac{Z}{a}\right)^{\frac{5}{2}} r\, e^{-\frac{Zr}{2a}}$ |
| 0 | 3 | $\dfrac{2}{3\sqrt{3}}\left(\dfrac{Z}{a}\right)^{\frac{5}{2}}\left(1-\dfrac{2Zr}{3a}+\dfrac{2Z^2 r^2}{27a^2}\right) e^{-\frac{Zr}{3a}}$ |
| 1 | 3 | $\dfrac{8}{27\sqrt{6}}\left(\dfrac{Z}{a}\right)^{\frac{3}{2}}\left(\dfrac{Zr}{a}-\dfrac{Z^2 r^2}{6a^2}\right) e^{-\frac{Zr}{3a}}$ |
| 2 | 3 | $\dfrac{4}{81\sqrt{30}}\left(\dfrac{Z}{a}\right)^{\frac{7}{2}} r^2 e^{-\frac{Zr}{3a}}$ |

The allowed energy in the radial wave function (equation 4.42) can be expressed as

$$E_n = -\left(\frac{Z^2 m e^4}{32\pi^2 \epsilon_0^2 \hbar^2}\right)\frac{1}{n^2} \qquad n = 0,1,2,\dots \tag{4.44}$$

The roles of quantum numbers in the Hydrogen atom are now clear. The principal quantum number, $n$, has values that range from $n = 1,2,3\dots$ It controls the range of values of $l = 0,1,2,\dots n-1$ and the overall energy in each orbital. The orbital angular momentum quantum number, $l$ denotes the shapes of the orbital. The magnetic quantum number, $m_l$, denotes the number of orbitals and their orientation within a subshell.

For a one electron wave functions in atoms are called atomic orbitals. Atomic orbitals with $l = 0$ are called *s-orbitals*, while $l = 1$, $l = 2$, and $l = 3$ are called *p-, d-,* and *f-orbitals*, respectively. These atomic orbitals can be represented by using energy sequence shown in Table 4.3 (Atkins et al., 2011).

Table 4.3 Orbitals

| $n$ | $l$ | Orbitals |
|-----|-----|----------|
| 1 | 0 | 1s |
| 2 | 0 | 2s |
| | 1 | 2p |
| 3 | 0 | 3s |
| | 1 | 3p |
| | 2 | 3d |

### 4.4. The Einstein Coefficient

Since the wave functions of $\Theta(\theta)$, $\Phi(\phi)$, and $R(r)$ have been calculated, Einstein A Coefficients can then be calculated by using equation 2.22.

In order to deal with the internal motion of the system, a reduced mass $\mu$ is introduced and it is defined as

$$\mu = \frac{m_e - m_N}{m_e + m_N} \tag{4.45}$$

where $m_e$ and $m_N$ are the electronic and nucleus mass with a value of $9.10304 \times 10^{-28} g$ for $\mu$ in this case. It is important to note that $\mu$ in the energy equation represents mass and is different from $\mu_{UL}$ in the Einstein A coefficient which represents the

transition dipole moment. The transition dipole moment is a three-dimensional integral where $\mu_{UL}$ and $M_{x,y,z}$ is a vector.

$$\overrightarrow{\mu_{UL}} = \int \Psi_U \overrightarrow{M_{x,y,z}} \Psi_L d\tau \tag{4.46}$$

where $M_{x,y,z} = e \cdot \vec{r}$ with $\vec{r} = \begin{bmatrix} x \\ y \\ z \end{bmatrix}$ in which $x, y, and\ z$ defines the direction of the moment and $e$ is the photon charge with the value of $1.6 \times 10^{-19} C = 4.8027 \times 10^{-10}$ statcoulombs. To calculate $\mu_{UL}$, two wave functions (upper level and lower level) must be considered, and the following comparison will consider an upper energy level of $2p$ $(n = 2, l = 1)$ and a lower energy level of $1s$ $(n = 1, l = 0)$.

$$|\mu_{UL}|^2 = |\mu_{x,UL}|^2 + |\mu_{y,UL}|^2 + |\mu_{z,UL}|^2 \tag{4.47}$$

To compute the wave function, the radial wave function and spherical wave function are needed. By multiplying both wave functions, the hydrogen wave function can be calculated.

$$\Psi(\theta, \phi, r) = Y(\theta, \phi) R(r) \tag{4.48}$$

Using equation 4.11, Table 4.1, and Table 4.2,

$$\Psi_{2p} = \frac{1}{4\sqrt{2\pi}} \left(\frac{Z}{a}\right)^{\frac{5}{2}} r e^{-\frac{Zr}{2a}} \cos\theta \tag{4.49}$$

$$\Psi_{1s} = \frac{1}{\sqrt{\pi}} \left(\frac{Z}{a}\right)^{\frac{3}{2}} e^{-\frac{Zr}{2a}} \tag{4.50}$$

Using the newly found wave functions, the transition dipole moment can be calculated. The transition dipole moment is calculated form the upper energy level to the lower energy level. Noting

$$x = r \, sin\theta \, cos \, \phi$$
$$y = r \sin \theta \sin \phi \qquad (4.51)$$
$$z = r \cos \theta$$

Since spherical coordinates are needed to simulate the hydrogen atom, therefore the differential volume will be in spherical coordinates.

$$d\tau = r^2 \sin \theta \, dr \, d\theta \, d\phi \qquad (4.52)$$

Using equation 4.49 and 4.50,

$$\mu_{x,UL} = \iiint \Psi_{2p} \cdot \Psi_{1s} \cdot ex \cdot d\tau \qquad (4.53)$$

$$\mu_{y,UL} = \iiint \Psi_{2p} \cdot \Psi_{1s} \cdot ey \cdot d\tau \qquad (4.54)$$

$$\mu_{z,UL} = \iiint \Psi_{2p} \cdot \Psi_{1s} \cdot ez \cdot d\tau \qquad (4.55)$$

Equation 4.59-4.61 can be separated into three integrals

$$\mu_{x,UL} = \frac{e}{4\pi\sqrt{2}} \int_{r=0}^{\infty} r^4 e^{-\frac{3Zr}{2a}} dr \int_{\theta=0}^{\pi} \cos\theta \, sin^2\theta \, d\theta \int_{\phi=0}^{2\pi} \cos\phi \, d\phi = 0 \qquad (4.56)$$

as $\int_{\phi=0}^{2\pi} \sin\phi \, d\phi = sin \, \phi \Big|_0^{2\pi} = 0$

$$\mu_{y,UL} = \frac{e}{4\pi\sqrt{2}} \int_{r=0}^{\infty} r^4 e^{-\frac{3Zr}{2a}} dr \int_{\theta=0}^{\pi} \cos\theta \, sin^2\theta \, d\theta \int_{\phi=0}^{2\pi} \sin\phi \, d\phi = 0 \qquad (4.57)$$

as $\int_{\phi=0}^{2\pi} \sin\phi \, d\phi = cos \, \phi \Big|_0^{2\pi} = 0$

$$\mu_{z,UL} = \frac{e}{4\pi\sqrt{2}} \int_{r=0}^{\infty} r^4 e^{-\frac{3Zr}{2a}} dr \int_{\theta=0}^{\pi} \sin\theta \; \cos^2\theta \; d\theta \int_{\phi=0}^{2\pi} d\phi = \frac{256 \cdot e \cdot a}{243Z\sqrt{2}} \quad (4.58)$$

where $a$ is the Bohr radius

By substituting the value,

$$\mu_{UL} = 1.8946 \times 10^{-18}$$

$$v = \frac{E}{h} = -\frac{Z^2 \mu e^4}{8\epsilon_0^2 h^3}\left(\frac{1}{n_U^2} - \frac{1}{n_L^2}\right) = 2.4652 \times 10^{-15} \; s^{-1}$$

$$A_{UL} = \frac{8\pi h v_{UL}^3}{c^3} \frac{|\mu_{UL}|^2}{6\epsilon_0 \hbar^2} = 6.2654 \times 10^8 \; s^{-1}$$

According to NIST (Sansonetti et al., n.d.) , $A_{UL}$ is $6.2659 \times 10^8 \; s^{-1}$

# 5. Matrix Formulations for the Hydrogen Atom

Analytical solutions do not exist for most problems. In this section, the Phi, Theta, and Radial equations are transformed into a matrix eigenvalue problem by using finite difference equations. This is done in order to develop computational procedures that can later be extended to more general problems. For the present problem, computations can be verified with the analytical solutions.

## 5.1. Phi Equation

A second order finite difference approximation to the second derivative is used in Equation (3.13).

$$\frac{\Phi_{i-1} - 2\Phi_i - \Phi_{i+1}}{\Delta\phi^2} = -m_l^2\Phi \tag{5.1}$$

Using equation 5.1 and the cyclic boundary condition (equation 4.4) which is being implemented on the first and last rows, the matrix eigenvalue problem can be constructed as follows

$$\frac{1}{\Delta\phi^2}\begin{bmatrix} -2 & 1 & 0 & & 0 & 0 & 1 \\ 1 & -2 & 1 & \ddots & \ddots & & 0 \\ \ddots & \ddots & \ddots & & \ddots & \ddots & 0 \\ 0 & \ddots & \ddots & & \ddots & \ddots & 0 \\ 0 & \dots & \dots & & 1 & -2 & 1 \\ 1 & 0 & 0 & & 0 & 1 & -2 \end{bmatrix}\begin{bmatrix} \\ \\ \phi \\ \\ \\ \end{bmatrix} = -m_l^2\begin{bmatrix} \\ \\ \phi \\ \\ \\ \end{bmatrix} \tag{5.2}$$

where the cyclic boundary condition is implemented on the first and last rows.

## 5.2. Theta Equation

By rearranging the basic governing equation, (3.13), and casting it in an operator notation

$$\left[\frac{\partial^2}{\partial\theta^2} + \frac{\cos\theta}{\sin\theta}\frac{\partial}{\partial\theta} - \frac{m_l^2}{sin^2\theta}\right]\Theta = -\lambda\Theta \tag{5.3}$$

As before we replace the derivatives with second order finite differences.

$$\left[\frac{\Theta_{i+1} - 2\Theta_i + \Theta_{i-1}}{\Delta\theta^2} + \frac{\cos\theta}{\sin\theta}\left(\frac{\Theta_{i+1} - \Theta_{i-1}}{2\Delta\theta}\right) - \frac{m_l^2\Theta_i}{sin^2\theta}\right] = -\lambda\Theta_i \tag{5.4}$$

Equation (5.4) then can be rearranged into a row of a matrix equation as

$$\left[\cdots \quad \frac{1}{\Delta\theta^2} - \frac{\cos\theta_i}{\sin\theta_i}\frac{1}{2\Delta\theta} \quad \frac{-2}{\Delta\theta^2} - \frac{m_\lambda^2}{\sin^2\theta_i} \quad \frac{1}{\Delta\theta^2} + \frac{\cos\theta_i}{\sin\theta_i}\frac{1}{2\Delta\theta} \quad \cdots\right]\begin{bmatrix} M \\ \Theta_{i-1} \\ \Theta_i \\ \Theta_{i+1} \\ M \end{bmatrix} = -\lambda\begin{bmatrix} M \\ \Theta_{i-1} \\ \Theta_i \\ \Theta_{i+1} \\ M \end{bmatrix} \tag{5.5}$$

All of the matrix coefficients have a term that becomes singular at the boundaries, *0* and *π*. Ostensibly, the problem can be eliminated by imposing Dirichlet conditions, *Φ(0)=Φ(π)=0*. Von Neumann conditions, *Φ'(0)=Φ'(π)=0* also will eliminate the singularities. Examples of these approaches are found throughout the literature. However, by inspection of the analytical solutions, $\Theta(\theta)$ and $\Theta'(\theta)$ go to finite values at the boundaries. These conditions are appropriate only for specific solutions. The matrix approach will return several solutions.

The first term on the left hand side of equation (5.3) is a second derivative, which can be evaluated using one-sided differences at the boundaries.

$$\frac{\partial \Theta}{\partial \theta} = \frac{-\frac{3}{2}\Theta_i + 2\Theta_{i+1} - \frac{1}{2}\Theta_{i+2}}{2\Delta\theta} \tag{5.6}$$

$$\frac{\partial^2 \Theta}{\partial \theta^2} = \frac{2\Theta_i - 5\theta_{i+1} + 4\Theta_{i+2} - \Theta_{i+3}}{\Delta\theta^2} \tag{5.7}$$

$$\frac{\partial \Theta}{\partial \theta} = \frac{-\frac{3}{2}\Theta_i + 2\Theta_{i-1} - \frac{1}{2}\Theta_{i-2}}{2\Delta\theta} \tag{5.8}$$

$$\frac{\partial^2 \Theta}{\partial \theta^2} = \frac{2\Theta_i - 5\Theta_{i-1} + 4\Theta_{i+2} - \Theta_{i-3}}{\Delta\theta^2} \tag{5.9}$$

The remaining terms, those with $sin\theta$ in the denominator, are extrapolated to the boundaries from the interior points, using a Taylor series. We define these terms as the function $F(\theta)$. At the lower, $i=1$ boundary, for example,

$$F_1 = F_2 - F_2'\Delta\theta + F_2''\frac{\Delta\theta^2}{2} - F_2'''\frac{\Delta\theta^3}{6} + H.O.T \tag{5.10}$$

The complete expansion of the theta equation can be found in Appendix A.

Matrix then can be constructed using finite difference equations for forward differencing (equations 5.12 and 5.13), backward differencing (equations 5.14 and 5.15), and central differencing (equation 5.7 and 5.8) which shown in equation 5.16.

$$
\begin{bmatrix}
\frac{2}{\Delta\theta^2}+f_1 & \frac{-5}{\Delta\theta^2}+f_1 & \frac{4}{\Delta\theta^2}+f_1 & \frac{-1}{\Delta\theta^2}+f_1 & & & & \\
\frac{1}{\Delta\theta^2}-\frac{\cos\theta_i}{\sin\theta_i}\frac{1}{2\Delta\theta} & \frac{-2}{\Delta\theta^2}-\frac{m_l^2}{\sin^2\theta_i} & \frac{1}{\Delta\theta^2}+\frac{\cos\theta_i}{\sin\theta_i}\frac{1}{2\Delta\theta} & \cdot & & & & \\
& \ddots & \ddots & & & & & \\
& & & & \ddots & \ddots & \ddots & \\
& & & & \frac{-1}{\Delta\theta^2}+f_1 & \frac{4}{\Delta\theta^2}+f_1 & \frac{-5}{\Delta\theta^2}+f_1 & \frac{2}{\Delta\theta^2}+f_1
\end{bmatrix}
\begin{bmatrix}\Theta\end{bmatrix}
\qquad (5.11)
$$

$$
= E \begin{bmatrix}\Theta\end{bmatrix}
$$

In the above $f_1$ denotes terms in the Taylor series expansion for $F_1(\theta)$, as in Appendix A.

## 5.3. Radial Equation

To compute the radial wave function numerically, equation 4.42 will be used. Upon substituting the finite difference formulas and rearranging, we have the matrix interior row equation.

$$
\left[-\frac{\hbar^2}{2m\Delta r^2}+\frac{\hbar^2}{2mr\Delta r}\right]R_{i-1}+\left[\frac{\hbar^2}{m\Delta r^2}+\frac{\lambda\hbar^2}{2mr^2}-\frac{Ze^2}{4\pi\epsilon_0 r}\right]R_i \qquad (5.12)
$$

$$
+\left[-\frac{\hbar^2}{2m\Delta r^2}-\frac{\hbar^2}{2mr\Delta r}\right]R_{i+1}=ER_i
$$

From the analytical solution by Atkins et al. and Levine, it is shown that a reasonable computational domain for the hydrogen atom is $30a_0$ where $a_0$ is the Bohr

Radius. Atkins et al compared the effective potential experienced by an electron in a hydrogen atom and concluded the range of the domain. Therefore the domain for $r$ in this particular problem is $0$ to $30a_0$. By using this domain, there will be a singularity, at $r = 0$, as we see in the second term in each of the brackets. In order to eliminate this singularity, the Taylor series extrapolation is used on the singular terms from the interior points. Note some are negative, and others positive; they tend to a finite number at $r=0$. Using the equation 5.10 from the previous subsection on the Taylor series extrapolation, the singular function can be written as

$$F(R) = -\frac{\hbar^2}{mr}R' + \left[\frac{\lambda\hbar^2}{2mr^2} - \frac{Ze^2}{4\pi\epsilon_0 r}\right]R \qquad (5.13)$$

One-sided differences are used on the boundaries as before. The complete derivation for the radial equation is in Appendix B. The matrix configuration for the radial equation is shown in equation 5.21. Note there are no extrapolated terms on the upper boundary.

$$\begin{bmatrix} \frac{-\hbar^2}{m\Delta r}+f_1 & \frac{5\hbar^2}{2m\Delta r^2}+f_1 & \frac{-2\hbar^2}{m\Delta r^2}+f_1 & \frac{\hbar^2}{2m\Delta r^2}+f_1 & \\ \frac{-\hbar^2}{2m\Delta r^2}+\frac{\hbar^2}{2mr\Delta r} & \frac{\hbar^2}{m\Delta r^2}+\frac{l(l+1)\hbar^2}{2mr^2}-\frac{Ze^2}{4\pi e_0 r} & \frac{-\hbar^2}{2m\Delta r^2}-\frac{\hbar^2}{2mr\Delta r} & \ddots & \\ & \ddots & & \ddots & \\ & & \frac{\hbar^2}{2m\Delta r^2} & \frac{-2\hbar^2}{m\Delta r^2} & \frac{5\hbar^2}{2m\Delta r^2} & \frac{-\hbar^2}{m\Delta r} \end{bmatrix}\begin{bmatrix} R \end{bmatrix} = E\begin{bmatrix} R \end{bmatrix}$$

$$(5.14)$$

## 6. Computational Results

Simulation results were obtained by developing the matrix (Section 5) in the code that was written in Fortran 95 for this thesis. Additionally, Lapack MKL library routines were used in order to compute the eigenvalues and the eigenfunction, while Matlab was used to calculate the wave function and for post processing. For all simulation results, a computational domain with 75 points was used for the Theta equation while 500 points were used for the Phi and Radial equation. A grid independence study was conducted to obtain a computational grid with adequate solution accuracy and low CPU and wall time. It is expected that the simulation results will be the same as the analytical solutions.

Few grids were attempted for the grid independence study; 10, 50, 100, 500, and 1000 grid points. It was found that the theta equation, 75 grid points were enough as the eigenvalue is the same as 50 and 100 grid points. However, when the eigenfunctions were compared with 75 grid points, the eigenfunctions were the same as 100 grid points but it was better than 50 grid points. For the phi equation, 500 grid points were needed as the eigenvalue and the eigenfunctions improved when compared to 400 grid points but did not improved after 500 grid points. For the radial equations, the eigenfunctions were plotted and compared between 50, 100, 500, and 1000 grid points. The result showed that the eigenfunctions did not improved after 500 grid points where the eigenvalue did not improve after 100 grid points. Therefore 500 grid points were used for the theta equation.

Table 6.1 shows the comparison of the results between the analytical and the numerical eigenvalue solutions of the Theta equation and Figure 6.1 to 6.5 shows a few numerical results compared against the analytical results of the eigenfunctions.

Table 6.1. Orbitals

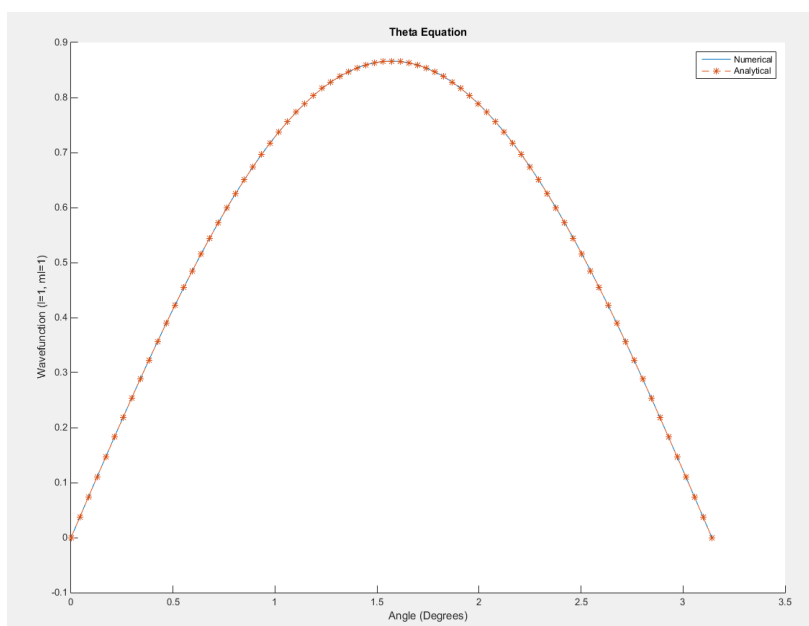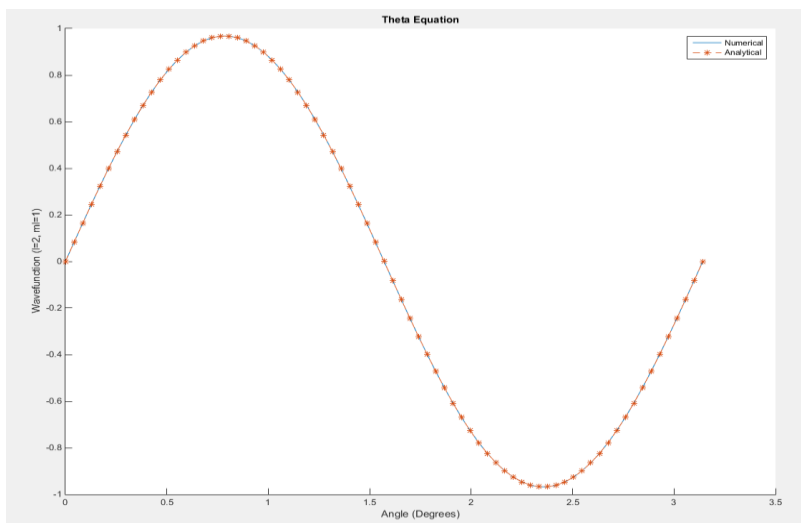| | Eigenvalues | | |
|---|---|---|---|
| $l$ | Numerical | Analytical | Percentage Error (%) |
| 0 | 0 | 0 | 0 |
| 1 | $-2.000$ | $-2$ | 0 |
| 2 | $-5.998$ | $-6$ | 0.03333 |
| 3 | $-11.99$ | $-12$ | 0.08333 |
| 4 | $-19.96$ | $-20$ | 0.2 |



Figure 6.1. Eigenfunctions of the Theta Equation: Analytical VS Numerical Results $l = 1, m_l = \pm 1$

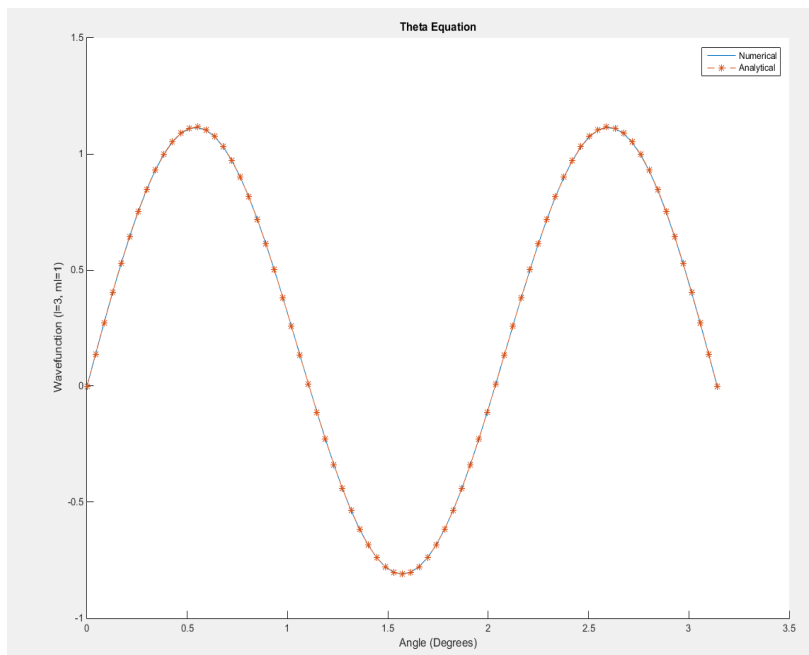Figure 6.2. Eigenfunctions of the Theta Equation: Analytical VS Numerical Results $l = 2, m_l = \pm 1$



Figure 6.3. Eigenfunctions of the Theta Equation: Analytical VS Numerical Results $l = 3, m_l = \pm 1$
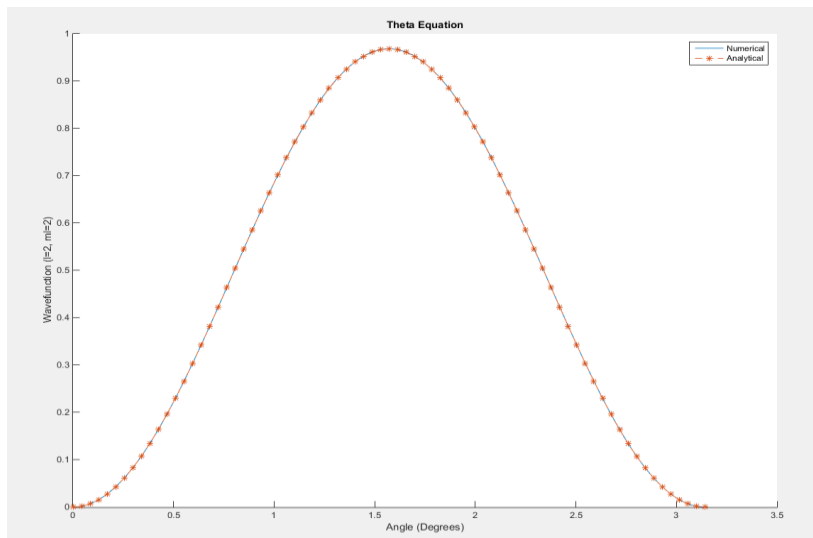
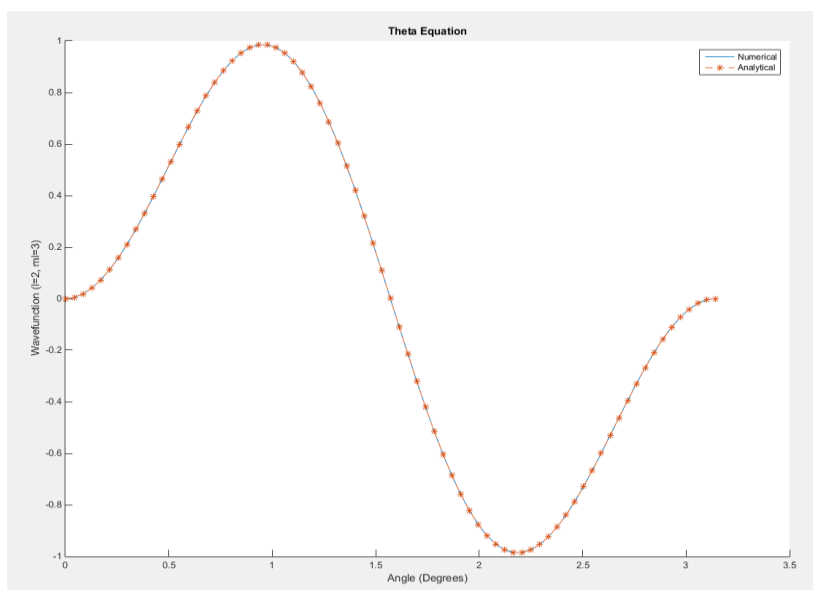Figure 6.4. Eigenfunctions of the Theta Equation: Analytical VS Numerical Results $l = 2, m_l = \pm 2$



Figure 6.5. Eigenfunctions of the Theta Equation: Analytical VS Numerical Results $l = 3, m_l = \pm 2$

Table 6.2 shows the comparison of the results between the analytical solutions and the numerical solutions of the Phi equation and Figure 6.6 to 6.10 shows few

numerical results compared against the analytical results of the eigenfunctions. From equation 4.12, it is shown that the results of the eigenfunctions contained real and imaginary components. However, by using LAPACK routine, the eigenfunctions that are computed includes the real components as well as the imaginary components of $\Phi$.

Table 6.2. Eigenvalues results of $\Phi(\phi)$

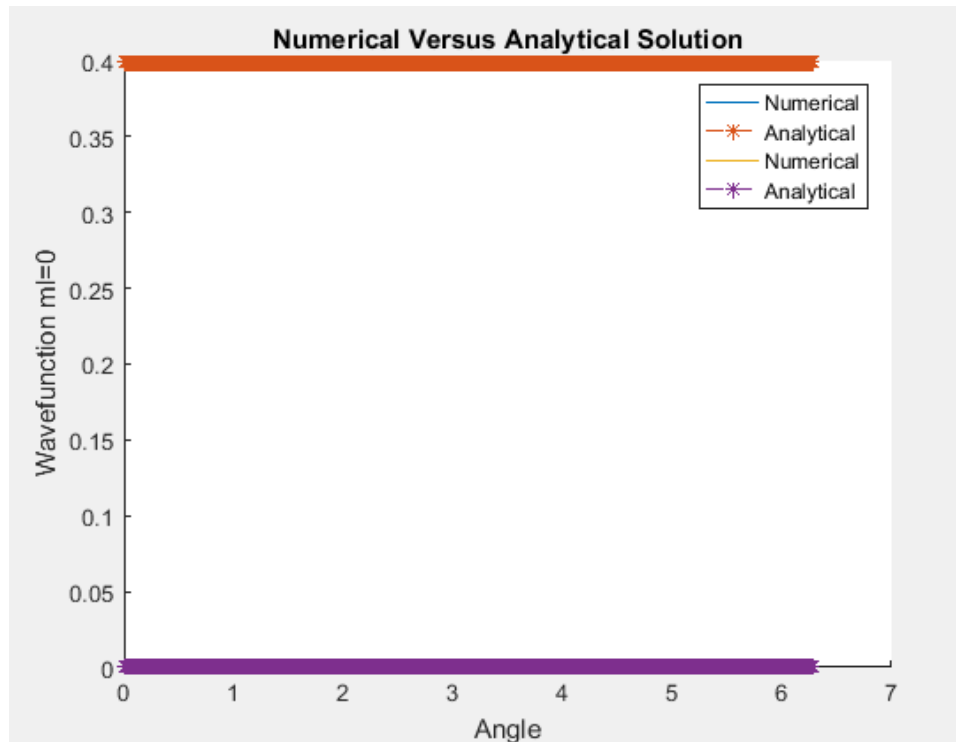| Eigenvalues | | | |
|---|---|---|---|
| $m_l$ | Numerical | Analytical | Percentage Error (%) |
| 0 | 0 | 0 | 0 |
| $\pm 1$ | $-1$ | $-1$ | 0 |
| $\pm 1$ | $-1$ | $-1$ | 0 |
| $\pm 2$ | $-3.998$ | $-4$ | 0.05 |
| $\pm 2$ | $-3.998$ | $-4$ | 0.05 |

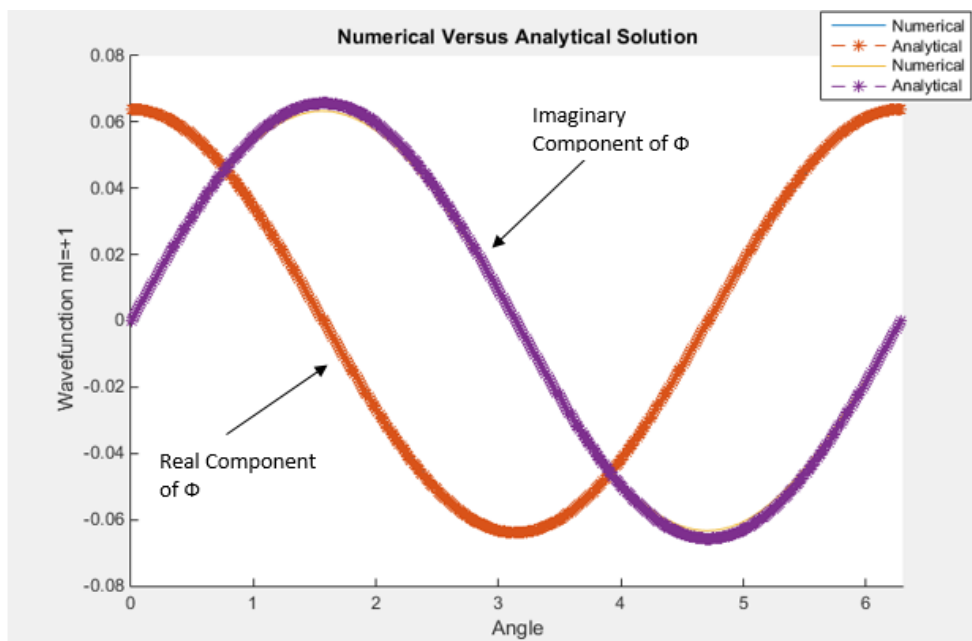Figure 6.6. Eigenfunctions of the Phi equation: Analytical VS Numerical Results (ml=0)



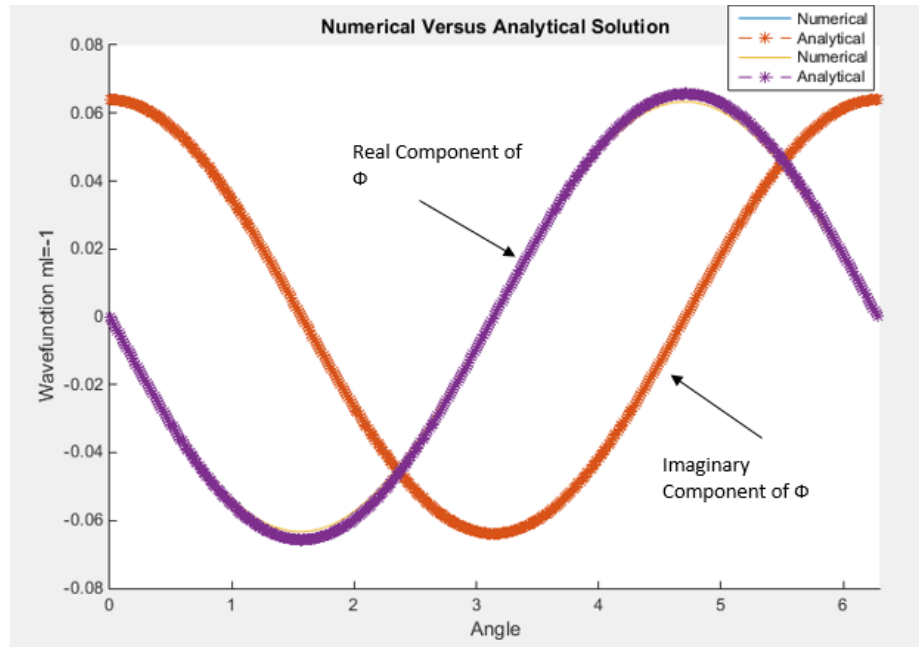Figure 6.7. Eigenfunctions of the Phi equation: Analytical VS Numerical Results (ml=+1)

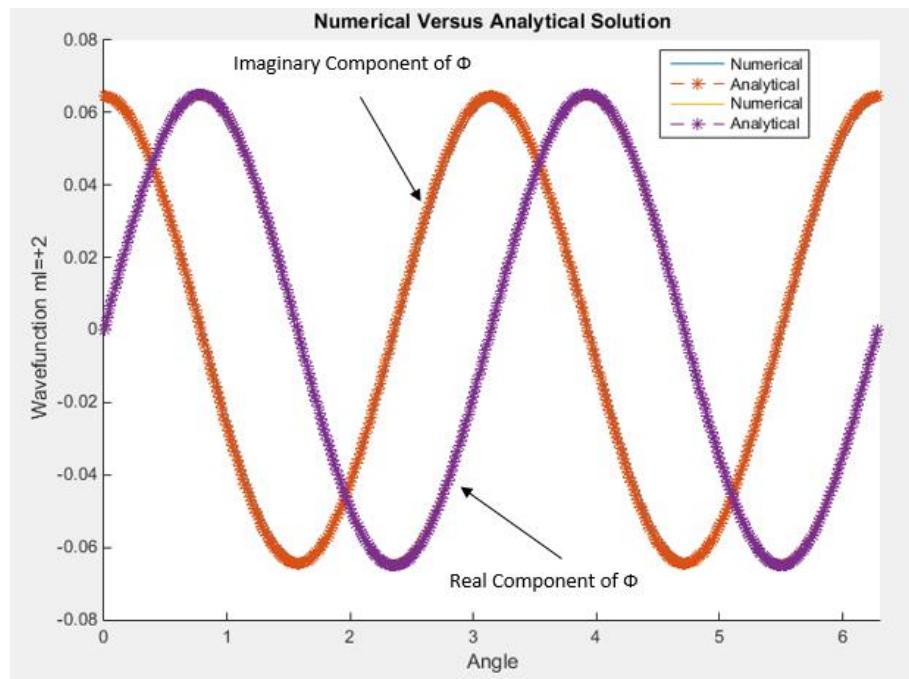Figure 6.8. Eigenfunctions of the Phi equation: Analytical VS Numerical Results (ml=-1)



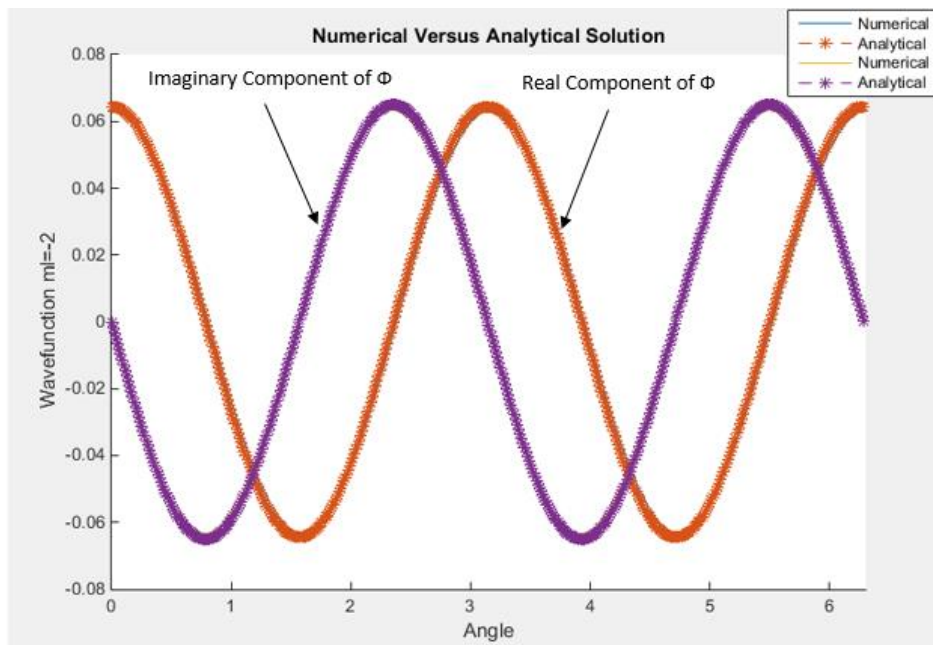Figure 6.9. Eigenfunctions of the Phi equation: Analytical VS Numerical Results (ml=+2)

Figure 6.10. Eigenfunctions of the Phi equation: Analytical VS Numerical Results (ml=-2)

Table 6.3 shows the comparison of the results between the analytical solutions and the numerical solutions of the Radial equation and Figure 6.11 to 6.16 shows few numerical results compared against the analytical results of the eigenfunctions.

Table 6.3. Eigenvalues results of R($r$)

| | Energy Eigenvalue | | |
|---|---|---|---|
| $n$ | Numerical | Analytical | Percentage Error (%) |
| 1 | $-0.2179e^{-10}$ | $-0.2179e^{-10}$ | 0 |
| 2 | $-0.5447e^{-11}$ | $-0.5448e^{-11}$ | 0.01835 |
| 3 | $-0.2417e^{-11}$ | $-0.2421e^{-11}$ | 0.2073 |
| 4 | $-0.1129e^{-11}$ | $-0.1362e^{-11}$ | 17.11 |



Figure 6.11. Eigenfunctions of the Radial Equation: Analytical VS Numerical Results
$(l = 0, n = 1, 1s)$

Figure 6.12. Eigenfunctions of the Radial Equation: Analytical VS Numerical Results
$(l = 0, n = 2, 2s)$



Figure 6.13. Eigenfunctions of the Radial Equation: Analytical VS Numerical Results
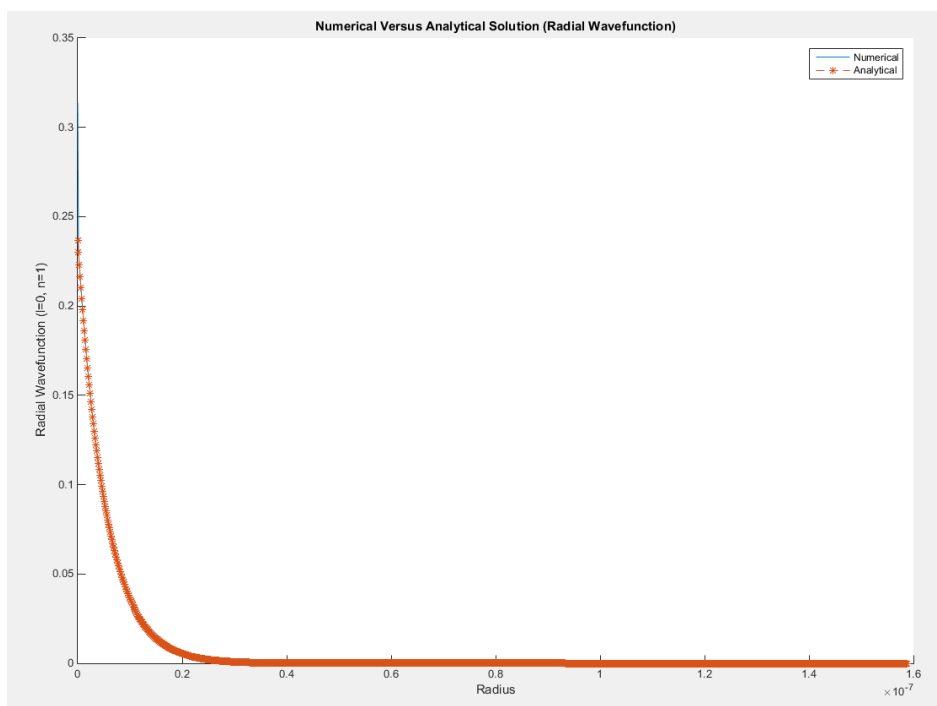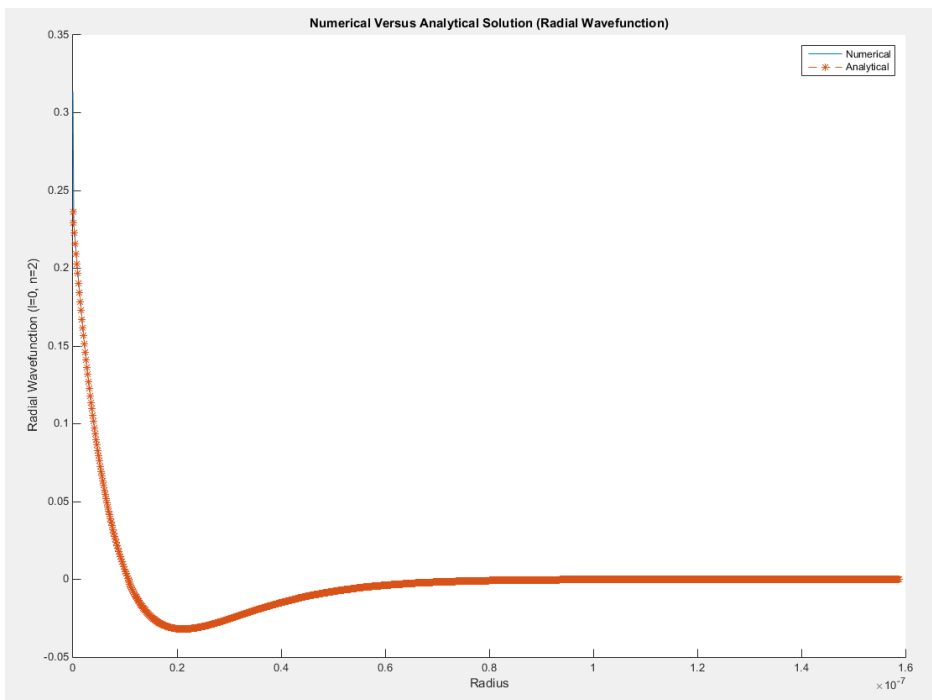$(l = 1, n = 2, 2p)$

Figure 6.14. Eigenfunctions of the Radial Equation: Analytical VS Numerical Results $(l = 0, n = 3, 3s)$
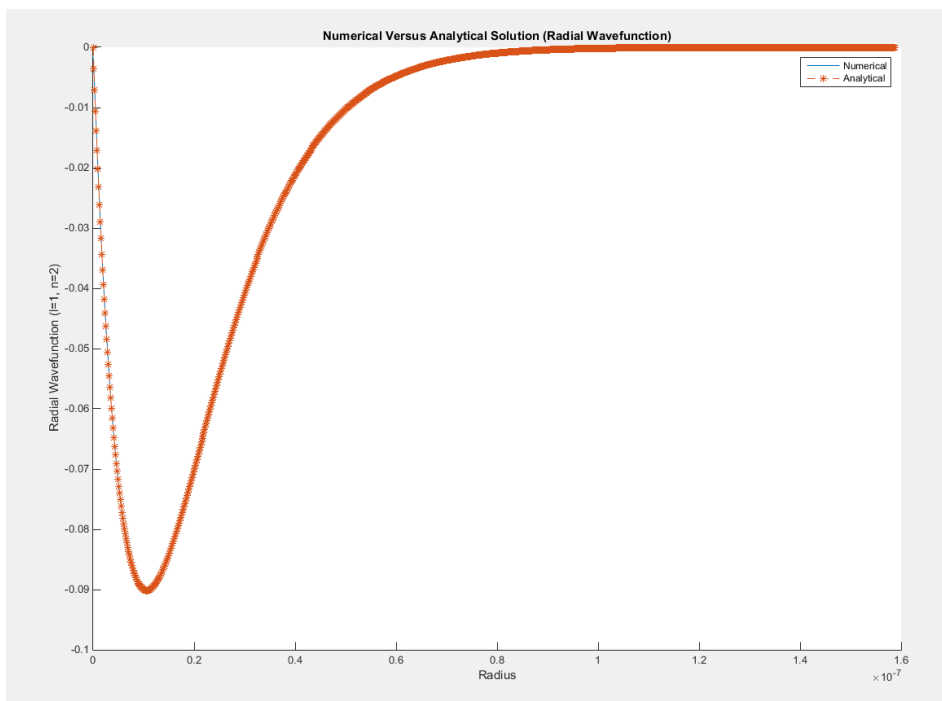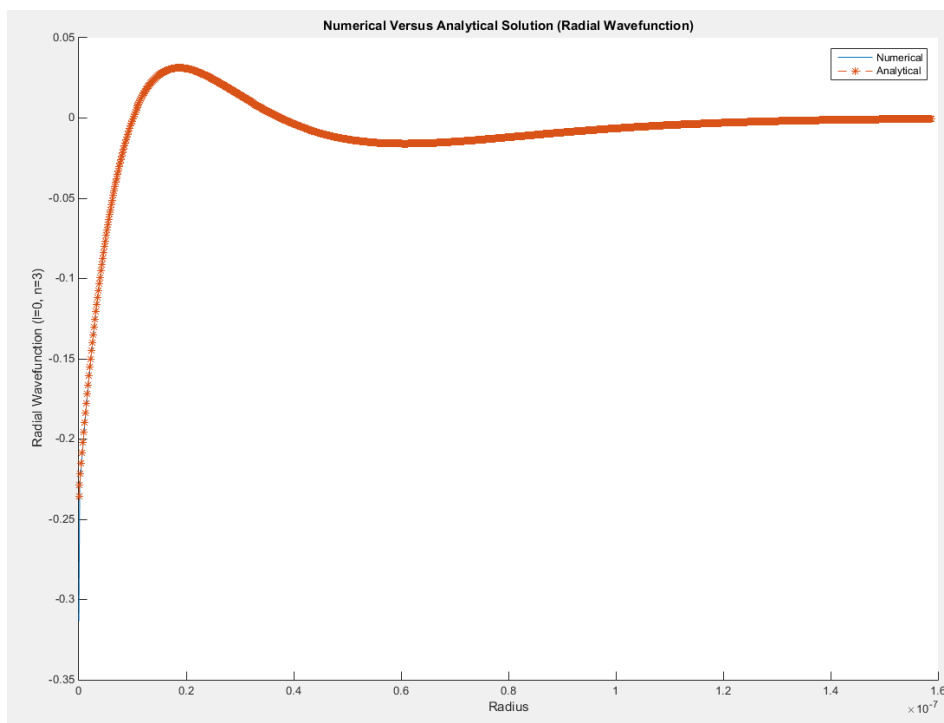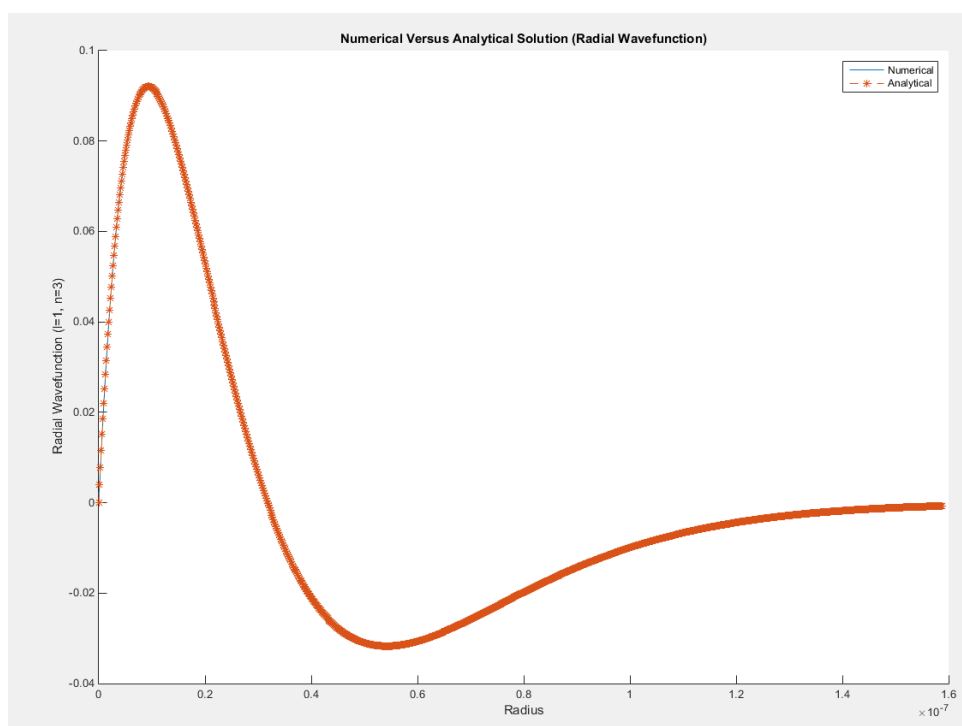


Figure 6.15. Eigenfunctions of the Radial Equation: Analytical VS Numerical Results $(l = 1, n = 3, 3p)$.
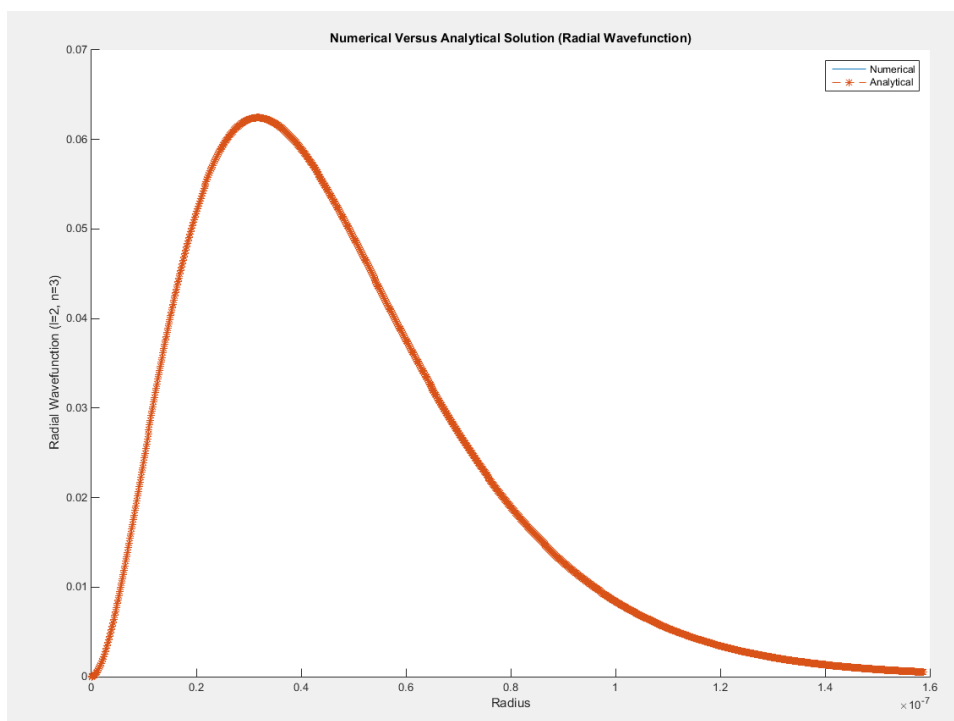
Figure 6.16. Eigenfunctions of the Radial Equation: Analytical VS Numerical Results $(l = 2, n = 3, 3d)$.

By using the wave functions that were computed, Einstein A coefficient then can be computed by using Matlab. It is used as post processing as it has a built in function that able to numerically integrate a .dat file where the all the eigenfunctions that were computed are stored. Table 6.4 shows both the analytical and the numerical results that were compared to the NIST (Sansonetti et al., n.d.) database for accuracy.

Table 6.4. NIST (Sansonetti et al., n.d.) Versus Numerical Result: Einstein A Coefficient

| Configurations | $A_{UL}$ (NIST) | $A_{UL}$ (Numerical) | Percentage Error (%) |
|---|---|---|---|
| $1s$ $2p$ | $6.2649 \times 10^8$ | $6.2565 \times 10^8$ | 0.1341 |
| $2s$ $3p$ | $3.7353 \times 10^8$ | $3.672 \times 10^8$ | 1.6946 |
| $1s$ $3p$ | $1.6725 \times 10^8$ | $1.6119 \times 10^8$ | 3.6233 |

By using the Einstein A Coefficient that has been computed, a lot of coefficients with interest to radiation problems then can be determined. One of the radiation properties that were used for this example is spontaneous spectral emission $\epsilon_\lambda$ ($\epsilon_\lambda = g_U N_U A_{UL} hc\phi_\lambda \frac{1}{4\pi\lambda}$).

Table 6.5. Spontaneous spectral emission comparison

| Configurations | $\epsilon_\lambda$ (NIST) | $\epsilon_\lambda$ (Numerical) |
|---|---|---|
| $1s$ $2p$ | $8.2020 \times 10^{12}$ | $8.1910 \times 10^{12}$ |
| $2s$ $3p$ | $1.3584 \times 10^{12}$ | $1.3354 \times 10^{12}$ |
| $1s$ $3p$ | $6.0822 \times 10^{11}$ | $5.8619 \times 10^{11}$ |

# 7. Conclusion

Figure 7.1 and Table 7.1 shows the percentage error comparison between $R(r), \Theta(\theta), and\ \Phi(\phi)$.
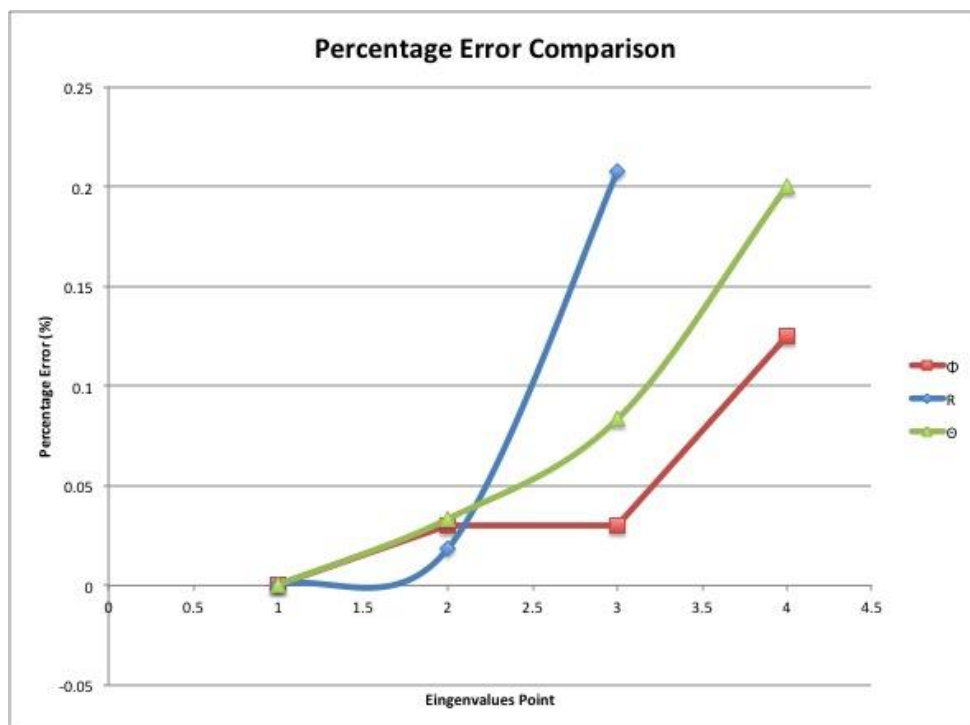


Figure 7.1. Percentage Error of the Eigenvalues

Table 7.1. Percentage Error of the Eigenvalues

| Eigenvalues | Percentage Error (%) | | |
|---|---|---|---|
| | $R(r)$ | $\Theta(\theta)$ | $\Phi(\phi)$ |
| 1st | $0.1e^{-18}$ | $0.1e^{-18}$ | $0.1e^{-18}$ |
| 2nd | 0.01835 | 0.03333 | 0.03 |
| 3rd | 0.2073 | 0.08333 | 0.03 |
| 4th | 17.11 | 0.2 | 0.125 |

Through comparing both the analytical and numerical solution, it shows that the matrix method is an accurate method to compute wave functions for lower energy levels and comparing the percentage error between $R(r), \Theta(\theta), and\ \Phi(\phi)$, it shows that as the energy level increase, the percentage error increase as well (Shown in Figure 7.1 and Table 7.1). However, the percentage error is significantly low, therefore it can be said that the matrix method is an acceptable and accurate method to compute both eigenvector and eigenvalue.

## 8. Future Work

Even though atomic hydrogen atom has been computed; in atmospheric re-entry there are different monatomic, diatomic, and polyatomic species. Therefore, for future work, a different monatomic atom can be analyzed using the matrix method and compare the results with NIST database. Diatomic molecules and polyatomic molecules can be analyzed too using the matrix method. In order to analyze diatomic molecules and polyatomic molecules, three-dimensional matrix need to be constructed. In addition, adaptive grid refinement can be applied to the model.

REFERENCES

Anderson, J. (2006). Hypersonic and high-temperature gas dynamics (2nd ed.). Reston, Va.: American Institute of Aeronautics and Astronautics.

Abramowitz, M. & Stegun, I. A., (1964). Handbook of Mathematical Functions With Formulas, Graphs, and Mathematical Tables. Applied Mathematics Series 55. Washington D.C., USA; New York, USA: United States Department of Commerce, National Bureau of Standards; Dover Publications.

Atkins, P. W. & Friedman, R.S., (2011) Molecular Quantum Mechanics (5th ed.). Oxford University Press.

Born, M., (1926), On the quantum Mechanics of Collision Processes. Quantum theory and measurement, section I.2., Princeton, New Jersey: Princeton University Press, 1983.

Brandis, A,N., Laux, C.O., Magin, T., McIntyre, T.J., & Morgan, R.G., (2014). Comparison of Titan Entry Radiation Shock-Tube Data with Collisional-Radiative Models. Journal of Thermophysics and Heat Transfer, 1-7.

Brandis, A.M., Johnston, C.O., Cruden, B.A., Prabhu, D., & Bose, D., (2011). Uncertainty Analysis of NEQAIR and HARA Predictions of Air Radiation Measurements Obtained in the EAST Facility. 42nd AIAA Thermophysics Conference, Fluid Dynamics and Co-located Conferences.

Brandis, A.M., Huo, W.M., & Johnston, C.O., (2013). Validation of HyperRad for Earth Entries. 44th AIAA Thermophysics Conference, Fluid Dynamics and Co-located Conferences, (AIAA 2013-2777)

Brandis, A.M., Johnston, C.O., Cuden. B.A., Prabhu, D.K., Wray, A.A., Liu, Y., Schwenke, D.W., & Bose, D., (2013). Validation of CO 4th positive radiation for Mars entry. Journal of Quantitative Spectroscopy and Radiative Transfer, Volume 121, May 2013, Pages 91-104.

Brazier-Smith, P. R., (1984). On the Limitations of Spherical Harmonics for the Solution of Laplace's Equation. Journal of Computational Physics 54, 524-530.

Einstein, A., (1917). On the Quantum Theory of Radiation. Physikalische Zeitschrift 18, 121

Fornberg, B., (1998). Calculation of Weights in Finite Difference Formulas. 1998 Society for Industrial and Applied Mathematics Vol. 40, No. 3, pp. 685-691, September 1998.

Howell, J. R., Pinar Menguc, M., & Siegel, R., (2015). Thermal Radiation Heat Transfer (6th ed). New York: Taylor & Francis, Inc.

Jaffe, R., (2014). Ab initio modeling of Molecular Radiation.

Johnston, C.O., Mazaheri, A., Gnoffo, P., Kleb, & B., Bose, D., (2013). Radiative Heating Uncertainty for Hyperbolic Earth Entry, Part 1: Flight Simulation Modeling and Uncertainty, Journal of Spacecraft and Rockets, Vol. 50, No. 1, pp. 19-38.

Khelashvili, A. A., & Nadareishvili, T. P., (n.d.). What is the Boundary Condition for the Radial Wave Function of the Schrödinger equation?

Levine, I. N., (2014). Quantum Chemistry (6th ed). Prentice Hall.

Prigara, F. V., (2003), Einstein's Coefficients and the Nature of Thermal Blackbody Radiation. Astron. Nachr., 324, No. S1, 425.

Salejda, W., Just, M., & Tyc, M. H., (2000). Numerical Matrix Method For Solving Stationary One-Dimensional Schrödinger Equation. AMSSE Program. Computational Methods in Science and Technology 6, 73-100.

Sansonetti, J., & Martin, W. (n.d.). Handbook of Basic Atomic Spectroscopic Data. Retrieved April, 2016, from http://www.nist.gov/pml/data/handbook/index.cfm

Schrödinger, E., (1926). An Undulatory Theory of the Mechanics of Atoms and Molecules. Physical Review 28 (6): 1049-1070.

Scholz, C., (2015). Modeling and Simulation of Radiation From Electronic Transitions in Hypersonic Atmospheric Reentry Flow,Master's Thesis, Embry –Riddle Aeronautical University.

Sohn, I. (2011). Modeling and Simulation from hypersonic flows with Monte Carlo methods.

Vincenti, W.G., Kruger, C.H. (1965). Introduction to physical gas dynamics, Robert E. Krieger Publishing Company.

Whiting, E.E., Park, C., Liu, Y., Arnold, J.O., & Paterson, J.A., (1996). NEQAIR96, Nonequilibrium and Equilibrium Radiative Transport and Spetra Program: User's Manual, Tech. rep., NASA Ames Research Center, Moffett Field, CA.

Wood, W.A., (2012). Radiation Coupling with the FUN3D Unstructured-Grid CFD code. 43rd AIAA Thermophysics Conference, Fluid Dynamics and Co-located Conferences (AIAA 2012-2741).

## A. Taylor Series Expansion of the Theta Equation

$$F(\theta) = \frac{\cos\theta}{\sin\theta}\Theta'(\theta) - \frac{m_l^2\Theta(\theta)}{\sin^2\theta}$$

$$F'(\theta) = \frac{\cos\theta}{\sin\theta}\Theta''(\theta) - \frac{1+m_l^2}{\sin^2\theta}\Theta'(\theta) + 2m_l^2\frac{\cos\theta}{\sin^3\theta}\Theta(\theta)$$

$$F''(\theta) = \frac{\cos\theta}{\sin\theta}\Theta'''(\theta) - \frac{2+m_l^2}{\sin^2\theta}\Theta''(\theta) + 2(1+2m_l^2)\frac{\cos\theta}{\sin^3\theta}\Theta'(\theta)$$

$$- 2m_l^2\frac{1+2cos^2\theta}{sin^4\theta}\Theta(\theta)$$

Taylor Series:

$$F_0 = F_1 - F_1'\Delta\theta - \frac{F_1''}{2}\Delta\theta^2 - \frac{F_1'''}{6}\Delta\theta^3+\ldots$$

$$\Delta\theta = \frac{\theta(\pi)}{Max\ Points - 1}$$

**<u>Upper Boundary ($\theta = 0, i = 1$):</u>**

Forward Differencing:

$$\Theta' = \frac{1}{\Delta\theta}\left[-\frac{3}{2}\theta_i + 2\theta_{i+1} - \frac{1}{2}\theta_{i+2}\right]$$

$$\Theta'' = \frac{1}{\Delta\theta^2}[2\theta_i - 5\theta_{i+1} + 4\theta_{i+2} - \theta_{i+3}]$$

$$\Theta''' = \frac{1}{\Delta\theta^3}\left[-\frac{5}{2}\theta_i + 9\theta_{i+1} - 12\theta_{i+2} + 7\theta_{i+3} - \frac{3}{2}\theta_{i+4}\right]$$

$$\theta = \Delta\theta$$

$$F_1 = \frac{\cos\theta}{\sin\theta}\frac{1}{\Delta\theta}\left[-\frac{3}{2}\theta_i + 2\theta_{i+1} - \frac{1}{2}\theta_{i+2}\right] - \frac{m_l^2\Theta_i}{\sin^2\theta}$$

$$F_1'\Delta\theta = \Delta\theta\left[\frac{\cos\theta}{\sin\theta}\frac{1}{\Delta\theta^2}[2\theta_i - 5\theta_{i+1} + 4\theta_{i+2} - \theta_{i+3}]\right.$$

$$\left.-\frac{1+m_l^2}{\sin^2\theta}\frac{1}{\Delta\theta}\left[-\frac{3}{2}\theta_i + 2\theta_{i+1} - \frac{1}{2}\theta_{i+2}\right] + 2m_l^2\frac{\cos\theta}{\sin^3\theta}\Theta_i\right]$$

$$\frac{F_1''}{2}\Delta\theta^2 = \frac{\Delta\theta^2}{2}\left\{\frac{\cos\theta}{\sin\theta}\frac{1}{\Delta\theta^3}\left[-\frac{5}{2}\theta_i + 9\theta_{i+1} - 12\theta_{i+2} + 7\theta_{i+3} - \frac{3}{2}\theta_{i+4}\right]\right.$$

$$-\frac{2+m_l^2}{\sin^2\theta}\frac{1}{\Delta\theta^2}[2\theta_i - 5\theta_{i+1} + 4\theta_{i+2} - \theta_{i+3}]$$

$$+ 2(1+2m_l^2)\frac{\cos\theta}{\sin^3\theta}\frac{1}{\Delta\theta}\left[-\frac{3}{2}\theta_i + 2\theta_{i+1} - \frac{1}{2}\theta_{i+2}\right]$$

$$\left.- 2m_l^2\frac{1+2\cos^2\theta}{\sin^4\theta}\Theta_i\right\}$$

**<u>Lower Boundary ($\theta = \pi, i = Max\ Points$):</u>**

Forward Differencing:

$$\Theta' = \frac{1}{\Delta\theta}\left[\frac{3}{2}\theta_i - 2\theta_{i-1} + \frac{1}{2}\theta_{i-2}\right]$$

$$\Theta'' = \frac{1}{\Delta\theta^2}[2\theta_i - 5\theta_{i-1} + 4\theta_{i-2} - \theta_{i-3}]$$

$$\Theta''' = \frac{1}{\Delta\theta^3}\left[\frac{5}{2}\theta_i - 9\theta_{i-1} + 12\theta_{i-2} - 7\theta_{i-3} + \frac{3}{2}\theta_{i-4}\right]$$

$$\theta = \pi - \Delta\theta$$

$$F_1 = \frac{\cos\theta}{\sin\theta}\frac{1}{\Delta\theta}\left[\frac{3}{2}\theta_i - 2\theta_{i-1} + \frac{1}{2}\theta_{i-2}\right] - \frac{m_l^2\Theta_i}{\sin^2\theta}$$

$$F_1' \Delta\theta = \Delta\theta \left[ \frac{\cos\theta}{\sin\theta} \frac{1}{\Delta\theta^2} [2\theta_i - 5\theta_{i-1} + 4\theta_{i-2} - \theta_{i-3}] \right.$$

$$\left. - \frac{1+m_l^2}{\sin^2\theta} \frac{1}{\Delta\theta} \left[ \frac{3}{2}\theta_i - 2\theta_{i-1} + \frac{1}{2}\theta_{i-2} \right] + 2m_l^2 \frac{\cos\theta}{\sin^3\theta} \Theta_i \right]$$

$$\frac{F_1''}{2} \Delta\theta^2 = \frac{\Delta\theta^2}{2} \left\{ \frac{\cos\theta}{\sin\theta} \frac{1}{\Delta\theta^3} \left[ \frac{5}{2}\theta_i - 9\theta_{i-1} + 12\theta_{i-2} - 7\theta_{i-3} + \frac{3}{2}\theta_{i-4} \right] \right.$$

$$- \frac{2+m_l^2}{\sin^2\theta} \frac{1}{\Delta\theta^2} [2\theta_i - 5\theta_{i-1} + 4\theta_{i-2} - \theta_{i-3}]$$

$$\left. + 2(1+2m_l^2) \frac{\cos\theta}{\sin^3\theta} \frac{1}{\Delta\theta} \left[ \frac{3}{2}\theta_i - 2\theta_{i-1} + \frac{1}{2}\theta_{i-2} \right] - 2m_l^2 \frac{1+2\cos^2\theta}{\sin^4\theta} \Theta_i \right\}$$

## B. Taylor Series Expansion of the Radial Equation

$$F = -\frac{\hbar^2}{m}\frac{R'}{r} + \frac{\lambda\hbar}{2m}\frac{R}{r^2} - \frac{Ze^2}{4\pi\varepsilon_0}\frac{R}{r}$$

$$F' = -\frac{\hbar^2}{m}\left[\frac{R''}{r} + \frac{-R'}{r^2}\right] + \frac{\lambda\hbar}{2m}\left[\frac{R'}{r^2} + \frac{-2R}{r^3}\right] - \frac{Ze^2}{4\pi\varepsilon_0}\left[\frac{R'}{r} + \frac{-R}{r^2}\right]$$

$$F'' = -\frac{\hbar^2}{m}\left[\frac{R'''}{r} - \frac{R''}{r^2} + \frac{2R'}{r^3} - \frac{R''}{r^2}\right] + \frac{\lambda\hbar}{2m}\left[\frac{R''}{r^2} - \frac{2R'}{r^3} - \frac{2R'}{r^3} + \frac{6R}{r^4}\right]$$

$$-\frac{Ze^2}{4\pi\varepsilon_0}\left[\frac{R''}{r} - \frac{R'}{r^2} - \frac{R'}{r^2} + \frac{2R}{r^3}\right]$$

Taylor Series:

$$F_0 = F_1 - F_1'\Delta r - \frac{F_1''}{2}\Delta r^2 - \frac{F_1'''}{6}\Delta r^3 + \dots$$

$$\Delta r = \frac{r(30a_0)}{Max\ Points - 1}$$

**Upper Boundary** $(r = 0, i = 1)$**:**

Forward Differencing:

$$R' = \frac{1}{\Delta r}\left[-\frac{3}{2}R_i + 2R_{i+1} - \frac{1}{2}R_{i+2}\right]$$

$$R'' = \frac{1}{\Delta r^2}[2R_i - 5R_{i+1} + 4R_{i+2} - R_{i+3}]$$

$$R''' = \frac{1}{\Delta r^3}\left[-\frac{5}{2}R_i + 9R_{i+1} - 12R_{i+2} + 7R_{i+3} - \frac{3}{2}R_{i+4}\right]$$

$$r = \Delta r$$

$$F_1 = -\frac{\hbar^2}{m}\frac{1}{r\Delta r}\left[-\frac{3}{2}R_i + 2R_{i+1} - \frac{1}{2}R_{i+2}\right] + \frac{\lambda\hbar}{2m}\frac{R_i}{r^2} - \frac{Ze^2}{4\pi\varepsilon_0}\frac{R_i}{r}$$

$$F_1' \Delta r = \Delta r \left\{ -\frac{\hbar^2}{m} \left[ \frac{1}{r\Delta r^2} (2R_i - R_{i+1} + 4R_{i+2} - R_{i+3}) \right. \right.$$

$$\left. -\frac{1}{r^2\Delta r} \left( -\frac{3}{2} R_i + 2R_{i+1} - \frac{1}{2} R_{i+2} \right) \right]$$

$$+\frac{\lambda\hbar}{2m} \left[ \frac{1}{r^2\Delta r} \left( -\frac{3}{2} R_i + 2R_{i+1} - \frac{1}{2} R_{i+2} \right) + \frac{-2R_i}{r^3} \right]$$

$$\left. -\frac{Ze^2}{4\pi\varepsilon_0} \left[ \frac{1}{r\Delta r} \left( -\frac{3}{2} R_i + 2R_{i+1} - \frac{1}{2} R_{i+2} \right) + \frac{-R_i}{r^2} \right] \right\}$$

$$\frac{F_1''}{2} \Delta r^2 = \frac{\Delta r^2}{2} \left\{ -\frac{\hbar^2}{m} \left[ \frac{1}{r\Delta r^3} \left( -\frac{5}{2} R_i + 9R_{i+1} - 12R_{i+2} + 7R_{i+3} - \frac{3}{2} R_{i+4} \right) \right. \right.$$

$$-\frac{1}{r^2\Delta r^2} (2R_i - 5R_{i+1} + 4R_{i+2} - R_{i+3})$$

$$+\frac{2}{r^3\Delta r} \left( -\frac{3}{2} R_i + 2R_{i+1} - \frac{1}{2} R_{i+2} \right)$$

$$\left. -\frac{1}{r^2\Delta r^2} (2R_i - 5R_{i+1} + 4R_{i+2} - R_{i+3}) \right]$$

$$+\frac{\lambda\hbar}{2m} \left[ \frac{1}{r^2\Delta r^2} (2R_i - 5R_{i+1} + 4R_{i+2} - R_{i+3}) \right.$$

$$-\frac{2}{r^3\Delta r} \left( -\frac{3}{2} R_i + 2R_{i+1} - \frac{1}{2} R_{i+2} \right) - \frac{2}{r^3\Delta r} \left( -\frac{3}{2} R_i + 2R_{i+1} - \frac{1}{2} R_{i+2} \right)$$

$$\left. +\frac{6R_i}{r^4} \right]$$

$$-\frac{Ze^2}{4\pi\varepsilon_0} \left[ \frac{R''}{r\Delta r^2} (2R_i - 5R_{i+1} + 4R_{i+2} - R_{i+3}) \right.$$

$$-\frac{1}{r^2\Delta r} \left( -\frac{3}{2} R_i + 2R_{i+1} - \frac{1}{2} R_{i+2} \right) - \frac{1}{r^2\Delta r} \left( -\frac{3}{2} R_i + 2R_{i+1} - \frac{1}{2} R_{i+2} \right)$$

$$\left. \left. +\frac{2R_i}{r^3} \right] \right\}$$

**Lower Boundary ($r = 30a_0, i = Max\ Points$):**

Forward Differencing:

$$R' = \frac{1}{\Delta r}\left[\frac{3}{2}R_i - 2R_{i-1} + \frac{1}{2}R_{i-2}\right]$$

$$R'' = \frac{1}{\Delta r^2}[2R_i - 5R_{i-1} + 4R_{i-2} - R_{i-3}]$$

$$R''' = \frac{1}{\Delta r^3}\left[\frac{5}{2}R_i - 9R_{i-1} + 12R_{i-2} - 7R_{i-3} + \frac{3}{2}R_{i-4}\right]$$

$$r = 30a_0 - \Delta r$$

$$F_1 = -\frac{\hbar^2}{m}\frac{1}{r\Delta r}\left[\frac{3}{2}R_i - 2R_{i-1} + \frac{1}{2}R_{i-2}\right] + \frac{\lambda\hbar}{2m}\frac{R_i}{r^2} - \frac{Ze^2}{4\pi\varepsilon_0}\frac{R_i}{r}$$

$$F_1'\Delta r = \Delta r\left\{-\frac{\hbar^2}{m}\left[\frac{1}{r\Delta r^2}(2R_i - 5R_{i-1} + 4R_{i-2} - R_{i-3})\right.\right.$$

$$\left.-\frac{1}{r^2\Delta r}\left(\frac{3}{2}R_i - 2R_{i-1} + \frac{1}{2}R_{i-2}\right)\right]$$

$$+\frac{\lambda\hbar}{2m}\left[\frac{1}{r^2\Delta r}\left(\frac{3}{2}R_i - 2R_{i-1} + \frac{1}{2}R_{i-2}\right) + \frac{-2R_i}{r^3}\right]$$

$$\left.-\frac{Ze^2}{4\pi\varepsilon_0}\left[\frac{1}{r\Delta r}\left(\frac{3}{2}R_i - 2R_{i-1} + \frac{1}{2}R_{i-2}\right) + \frac{-R_i}{r^2}\right]\right\}$$

$$\frac{F_1''}{2}\Delta r^2 = \frac{\Delta r^2}{2}\left\{-\frac{\hbar^2}{m}\left[\frac{1}{r\Delta r^3}\left(\frac{5}{2}R_i - 9R_{i-1} + 12R_{i-2} - 7R_{i-3} + \frac{3}{2}R_{i-4}\right)\right.\right.$$

$$-\frac{1}{r^2\Delta r^2}(2R_i - 5R_{i-1} + 4R_{i-2} - R_{i-3}) + \frac{2}{r^3\Delta r}\left(\frac{3}{2}R_i - 2R_{i-1} + \frac{1}{2}R_{i-2}\right)$$

$$\left.-\frac{1}{r^2\Delta r^2}(2R_i - 5R_{i-1} + 4R_{i-2} - R_{i-3})\right]$$

$$+\frac{\lambda\hbar}{2m}\left[\frac{1}{r^2\Delta r^2}(2R_i - 5R_{i-1} + 4R_{i-2} - R_{i-3})\right.$$

$$\left.-\frac{2}{r^3\Delta r}\left(\frac{3}{2}R_i - 2R_{i-1} + \frac{1}{2}R_{i-2}\right) - \frac{2}{r^3\Delta r}\left(\frac{3}{2}R_i - 2R_{i-1} + \frac{1}{2}R_{i-2}\right) + \frac{6R_i}{r^4}\right]$$

$$-\frac{Ze^2}{4\pi\varepsilon_0}\left[\frac{R''}{r\Delta r^2}(2R_i - 5R_{i-1} + 4R_{i-2} - R_{i-3})\right.$$

$$-\frac{1}{r^2\Delta r}\left(\frac{3}{2}R_i - 2R_{i-1} + \frac{1}{2}R_{i-2}\right) - \frac{1}{r^2\Delta r}\left(\frac{3}{2}R_i - 2R_{i-1} + \frac{1}{2}R_{i-2}\right)$$

$$\left.\left.+\frac{2R_i}{r^3}\right]\right\}$$